

We are IntechOpen, the world's leading publisher of Open Access books Built by scientists, for scientists

4,800

Open access books available

122,000

International authors and editors

135M

Downloads

Our authors are among the

154

Countries delivered to

TOP 1%

most cited scientists

12.2%

Contributors from top 500 universities



WEB OF SCIENCE™

Selection of our books indexed in the Book Citation Index
in Web of Science™ Core Collection (BKCI)

Interested in publishing with us?
Contact book.department@intechopen.com

Numbers displayed above are based on latest data collected.

For more information visit www.intechopen.com



Microsensors for Microreaction and Lab-on-a-chip Applications

Pawel Knapkiewicz and Rafal Walczak
*Wroclaw University of Technology
Poland*

1. Introduction

Since the first successful applications of the microfluidical devices, measurement of physical, chemical and biochemical parameters of performed reactions and analysis became next challenge and millstone towards successful application of developed instrumentation in many field of science and industry, as well as, deeper understating of micro- and nano-world of fluidics (Ehrfeld at al., 2005). Although, methodology of these measurements was well known from many years, the main problems that occurred were dimensional incompatibility of available macroscopic solutions and sensing problems caused by significant reduction of managed and analyzed volumes. Therefore, microsensors became important part of the microfluidical device enabling real-time and on-chip measurement of measurable parameters like pressure, temperature, conductivity, absorbance or fluorescence.

In this chapter miniature on-chip integrated pressure sensors, discreet corrosion resistant pressure sensor and conductometric flow-through detector will be described in details. Nevertheless, optical microsensors like absorbance NIR and VIS detector, as well as fluorometric detector will be shown. Technology of the sensors utilizes microengineering techniques where silicon and glass play main role as constructional materials. Three-dimensional formation and assembling techniques of silicon and glass allow to fabricate miniature sensors. For each presented microsensor, the fabrication techniques will be described in details. Great attention is also paid for development of the complete measurement system consisting of the microsensors itself but also specialized electronics and information environment for full data management and measurement or analyse result presentation.

2. Miniature sensors and measurement systems for microreaction technology

Pressure and temperature are two the most important parameters of chemical reactions. Steering of those parameters determine chemical reaction course, as well as temperature and pressure inform about actual chemical reaction state. Continues monitoring of temperature and pressure is very important for exothermic, high-speed chemical reactions (Edited by Dietrich, 2009). It can be done relatively easy for standard, macro-scale chemical plants. Commercially available sensors are suitable to large apparatus, can be easy applied and

operate as a part of some automation systems. The microreaction technology stays in opposite to this situation. Chemical reactions are performed in the microscale by the use of microreactors, replacing static chemical reactions by continuous-flow reactions. Unfortunately, there is no ready-to-use sensors suitable to the microreactors. Total inner volume of the microreactors is in the range from several μl to few ml, when external dimensions, as well as "dead" volume of available standard sensors are at least ten times larger, in comparison. In consequence, commercially available sensors can not work in tandem with the microreactors.

Let's focus our attention on extremely dangerous, highly exothermic chemical reaction, eg. nitration of organic compounds (Ali et al., 2005; Speight, 2002), where continuous monitoring of pressure and temperature inside the microreactor is absolutely required from safety point of view. Moreover, real-time measured data are helpful for conscious steering of chemical reaction, towards high yield (Kralish & Kreisel, 2007).

In this paragraph miniature temperature and pressure sensors, as well as measurement systems dedicated to the microreaction technology will be described. Several requirements of parameters of the sensors and sensors assembling method must be considered:

- temperature sensors operating range: $-20^{\circ}\text{C} \div +100^{\circ}\text{C}$,
- dimensions of the temperature sensors should not exceed typical dimensions of microchannels (typical dimensions are in range of tens μm up to several mm - the average is 1 mm),
- pressure sensors operating range: relative pressure 0 kPa \div 400 kPa, overpressure up to 600 kPa,
- "dead" volume of all pressure sensors integrated to microreactor should not exceed 1/10 of total inner volume of microreactor,
- microreactor with sensors work in harsh environment (concentrated acids, organic compounds),
- chemically resistance assembling required.

In the current paragraph hole process, including temperature sensors selection, pressure sensors development, assembling and packaging problems, as well as electronics and software realization, towards complete sensoric system for microreaction technology, will be described in details.

2.1 Temperature sensors

Temperature sensors working in a tandem with microreactor must be characterized by small dimensions, fast response and small measurement error. Sensor can be localised inside microchannel (direct contact to medium) or outside microchannel (indirect contactless measurement).

Direct sensor-to-medium contact gives most precision measurement. Thin film sensors evaporated onto inner walls of microchannel will not survive aggressive chemicals. Moreover, thin film technology is difficult. Discrete temperature sensors can be assembled in the microchannel only by gluing. Both ideas do not fulfil previously listed requirements, what in consequence eliminates this measurement idea and technical realization from the use.

Second method is based on sensor localized outside microchannel. Main requirement is to keep distance between sensor and medium as small as possible to allow to conduct a heat flux with minimum losses.

Several types of commercially available sensors can be investigated. Main parameters of commercially available sensors are collected in Table 1.

| Parameter Type/model | Operating range | Output signal | Tolerance | Housing/Dimensions |
|-------------------------------------|---|---|---------------|--|
| Pt100 / Pt500 / Pt1000 | -200°C ÷ +860°C (depending on type) | Resistance, linear PTC ¹ | ≤ 0.3% | SMD ² 0805, SMD 1206, TO92, SOT223, ceramic or metal tube ø ≥ 1.5 mm, other |
| Thermistor NTC | -55°C ÷ +150°C (depending on type) | Resistance, non-linear NTC ³ | 1% ÷ 10% | SMD 0603, SMD 0805, pill- like ø ≥ 0.8 mm |
| Thermocouples | -200°C ÷ +1820°C (depending on type) | Voltage, linear | ±0.5°C ÷ ±4°C | metal tube ø ≥ 0.15 mm |
| Transducers with analogue output | -55°C ÷ +155°C (depending on type) | Voltage, linear (usually) | 0.5% ÷ 5% | all electronic standards |
| Transducers with digital output | -55°C ÷ +155°C (depending on type) | digital, serial data transfer | 0.5% ÷ 5% | all electronic standards |

Table 1. Temperature sensors and their main parameters

The most common are transducers with analogue output. Output voltage signal is linear in relation to the measured temperature and easy to measure. No additional electronic circuits are required to process the signal. Second, most useful are transducers with digital output. The only difference to previous one is, that digital processing by a microcontroller is required. Unfortunately, even the smallest package of temperature transducers (SOT23 electronic standard, plastic body dimensions without electrical connections: 2.9 × 1.3 × 0.85 mm³) seems to be too large to be directly applied in microreaction technology (Fig. 1a).

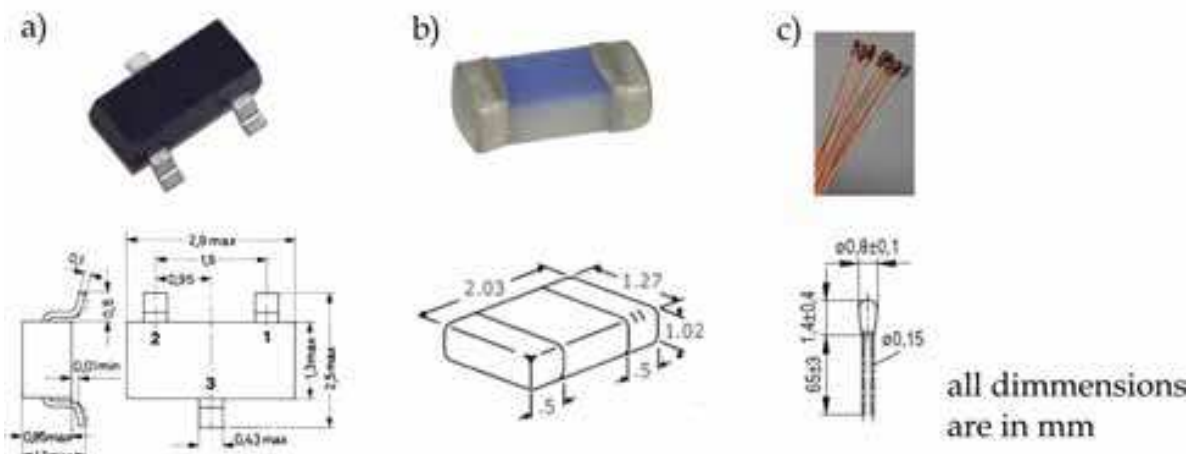


Fig. 1. Examples of miniature temperature sensors: a) temperature transducer in SOT23 package, b) PTC platinum thermoresistor (Pt-series) at 0603 SMD package, c) pill-like NTC thermistor

¹ PTC – Positive Thermal Coefficient

² SMD – Surface Mounted Devices

³ NTC – Negative Thermal Coefficient

Different packages and dimensions of resistance PTC or NTC sensors and thermocouples are available. Platinum temperature sensors (Pt-series) are very accurate and are used as temperature standards. Dimensions of the ceramic or metal tube packages, as well as SMD packages, do not fulfil harsh-environment microreaction requirements (Fig. 1b). NTC thermistors are available in different SMD packages, including miniature pill-like packages distinctive from others (Fig. 1c). The smallest pill-like package has 0.8 mm diameter, what is suitable to mentioned earlier requirements. Thermocouples are usually packaged in the metal tubes. Special constructions are available in tubes of 0.15 mm in diameter. It is the smallest dimension (diameter) of all sensors discussed before. In spite of that, thermocouples need to co-work with sophisticated electronic circuits.

The analysis of commercially available temperature sensors appoints that the miniature pill-like NTC thermistors as the best solution. Small glass package, thin and flexible electrical wires entail small thermal capacity and fast response.

The location of miniature pill-like NTC thermistors onto microreactors made of glass, silicon and glass as cover, ceramics, polymers, was proposed. Sensor should be located inside “blind” hole of 1.0 mm in maximum diameter, fabricated directly above microchannel. The optimal distance of 200 μm between medium and temperature sensor has been found experimentally to be optimal. The schematic cross-section of a microreactor with NTC thermistor and the sensor integration to glass-silicon-glass microreactor is schematically presented on Fig. 2.

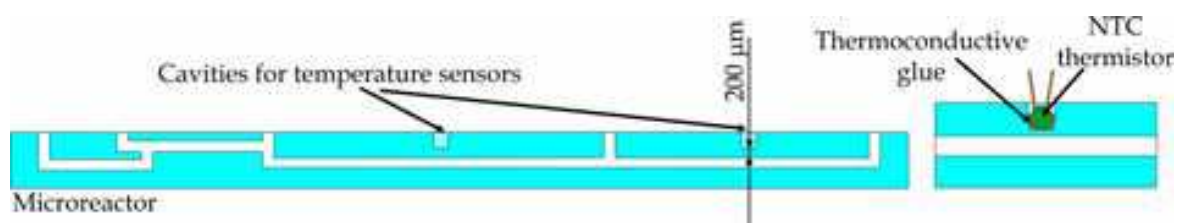


Fig. 2. Indirect temperature measurement: cross-section of a microreactor (left) and NTC thermistor location (right)

Thermal behaviours of the glass-silicon-glass microreactor equipped with miniature pill-like NTC thermistors will be widely discussed later in paragraph 2.3.

2.2 Pressure sensors

As it was mentioned before, required operation range of pressure sensors is from 0 kPa to 400 kPa of relative pressure. 400 kPa is a maximum operating pressure of microreactors made of glass, silicon-glass, ceramics and polymers, in most cases.

Pressure sensor must have direct contact to a measured medium. The “dead” volume of all applied pressure sensor must be as small as possible, in order to do not influence on chemical reaction conducted inside microchannels. The assumption, that “dead” volume of all pressure sensors V_{DV} should not exceed 1/10 of total inner volume of microreactor V_{MR} (1) is appropriate from metrological point of view and minimize negative influence on chemical reaction.

$$1/10 V_{MR} > V_{DV} \quad (1)$$

The “dead” volume of commercially available pressure sensors and transducers (dedicated to harsh environment chemical plants) is counted in mili-litres. Moreover, large size packages disqualify these pressure sensors to be used in the microreaction technology (Fig. 3).



Fig. 3. Examples of commercially available pressure transducers (Peltron, Poland) with stainless steel separation membrane: a) NPX series, b) PXW series with LED display, c) PXC series with additional separation membrane dedicated to harsh environment measurements.

Two variants of pressure measurements inside microchannels have been taken into considerations. The first strategy is to integrate the pressure sensors directly onto microreactor. The second strategy is to use discreet sensors which are independent on the microreactor.

2.2.1 Miniature pressure sensor integrated onto microreactors

Some pre-work tests of chemical resistance of some possible to use assembling methods have been done. Test structures consist of 3" silicon and glass wafers were bathed in H₂SO₄+HNO₃ mixture 1:1 (Table 2).

| Assembling method | Gluing - photo-hardened glue | Gluing - epoxy glue | Adhesive bonding - Kapton® foil (DuPont) | Adhesive bonding - Teflon foil (DuPont) | Silicon-to-glass anodic bonding |
|--|------------------------------|---------------------|--|---|---------------------------------|
| Test: bathed in H ₂ SO ₄ +HNO ₃ mixture | - | - | - | - | + |

Table 2. Resistance against aggressive chemicals of chosen assembling methods

The test shows, that any kind of gluing and adhesive bonding can not be use. Only silicon-to-glass anodic bonding ensures strong, tight and chemically resistant connection. The selected assembling method can by utilized only for glass or silicon-glass microreactors. Moreover, only borosilicate glass (Pyrex-like) can be used (Briand at al., 2004; Knapkiewicz at al., 2007; Dziuban, 2006).

Two ways to integrate pressure sensors directly to the microreactor are possible. Silicon piezoresistive pressure sensor dies are anodically bonded to a top glass cover of the microreactor or sensor dies onto glass posts are integrated to a top glass cover of microreactor trough silicon orifice in two steps of anodic bonding (Fig. 4).

The "dead" volume of two proposed solutions, including "dead" volume of connection channel trough top glass cover, has been estimated assuming 1.1 mm thickness of top glass cover and hole of 0.7 mm in diameter. The "dead" volume is equal to 0.75 µl and 1.65 µl, respectively. The second solution has larger "dead" volume. In spite of that, mechanical

stress indication at silicon sensor die (false signal) is less possible in comparison to the solution with dies bonded directly to the microreactor top cover.

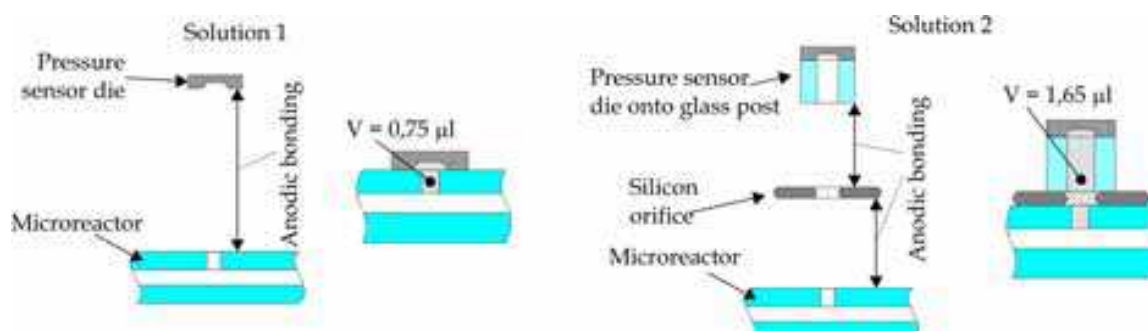


Fig. 4. Two solutions of pressure sensors assembling.

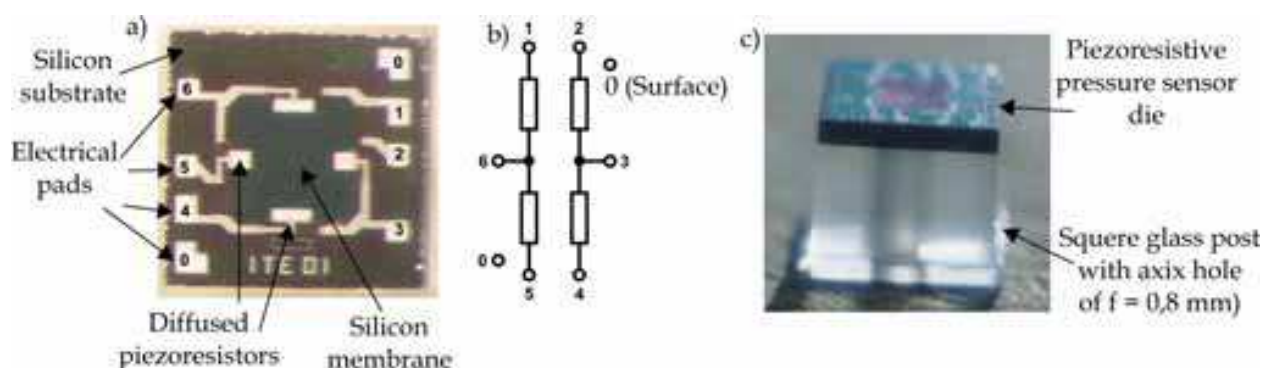


Fig. 5. Silicon piezoresistance pressure sensor (ITE Warsaw): a) top view of the silicon die, b) Wheatston bridge configuration of the piezoresistors, c) silicon die onto glass post

Silicon piezoresistive pressure sensor structures (silicon sensor die on glass post) fabricated at Institute of Electron Technology in Warsaw (ITE Warsaw), has been chosen (Fig. 5). Basic parameters of the sensors are collected in Table 3.

| Parameters | Required value | Catalogue value of ITE Warsaw pressure sensors |
|------------------------|----------------|--|
| Nominal pressure | 600 kPa | 600 kPa |
| Static overpressure | max 300 kPa | min 400 kPa* |
| Dynamic overpressure | - | min 750 kPa* |
| Total error | < 1% | < 0,5% |
| Work temperature range | - 10°C ÷ 40°C | 0°C ÷ 50°C |
| Response time | < 100 ms | < 1 ms |

Table 3. Comparison of requirements and catalogue values of ITE Warsaw pressure sensors

2.2.2 Glass-silicon-glass microreactor with on-chip integrated temperature and pressure sensors

Validation of the concept of temperature and pressure sensors integration was provided by fabrication of the demonstrator of a packaged microreactor made of silicon and Pyrex-like glass (Knapkiewicz et al., 2006). The microreactor has integrated 4 pressure sensors dies and 5 temperature sensors. The silicon pressure sensors dies on 2 mm high Pyrex-like glass post

are anodically bonded to the silicon orifice, which is anodically bonded to the glass-silicon-glass microreactor in the next step. Via-holes connecting fluidic channel of the microreactor and pressure sensors, as well as blind-holes for positioning of temperature sensors, are made in proper places of the microreactor (Fig. 6).

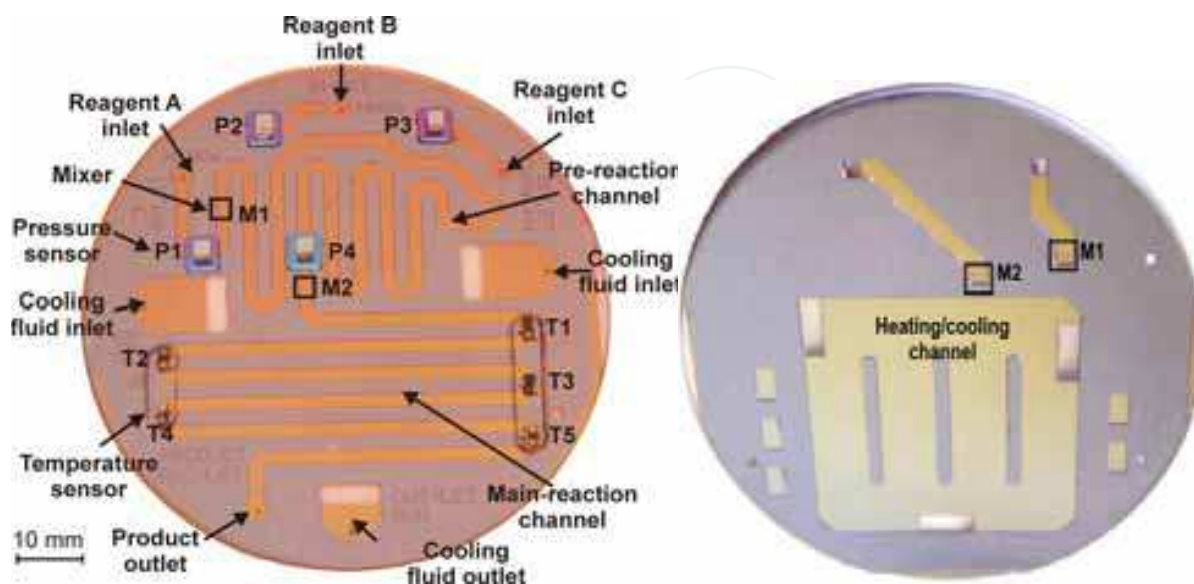


Fig. 6. Silicon-glass microreactor with on-chip integrated pressure and temperature sensors: top (left) and bottom view (right) of assembled microreactor

The microreactor is made of three layers of glass, silicon and glass (Fig. 7). The microfluidical channels (2 mm wide, 120 μm depth), the structure of two micromixers (10 micronozzles of 50 x 50 μm^2 each one) and the cooling chamber are formed by a deep, wet micromachining of (100)-oriented, double-side polished silicon wafer in 40% KOH solution at 80°C. Inner volume of the microreactor has been estimated to be 143 μl . “Dead” volume of the four pressure sensors is 5.7% of the microreactor volume, what is suitable to assumption (1).

After micromachining the microreactor body is oxidized to form 0.3 μm - thick silicon dioxide chemically resistive layer. Following, the body is anodically bonded (450°C, 1.5 kV) to the bottom glass substrate (Borofloat 3.3, Schott, Germany). Next, the top glass with set of pressure sensors is prepared. Firstly, via holes ($\varnothing = 0.7$ mm) of fluidic inlets, outlets and pressure sensors connections are mechanically drilled in the top glass. Next, cavities ($\varnothing = 1.0$ mm) for temperature sensors are mechanically drilled. Piezoresistive pressure sensor dies on 2 mm-high glass post (Borofloat 3.3) are anodically bonded to the previously micromachined 5 x 5 mm² silicon orifices with via holes (Fig. 7a). The silicon orifices are wet-etched in a separate process. After that, sensor dies with silicon orifices are anodically bonded to the top glass. Such construction of the sensor module eliminates temperature induced stresses and, in consequence, temperature induced errors. It ensures excellent tightness of the fluidic connections. Finally, the top glass with pressure sensors is anodically bonded (450°C, 1 kV) to the microreactor silicon body (Fig. 7b).

The miniature pill-like thermistors (NTC, 5 k Ω , EPCOS) are positioned inside cavities and fixed by the use of thermo-conductive glue. The distance between the sensor and main reaction channel is below 200 μm .

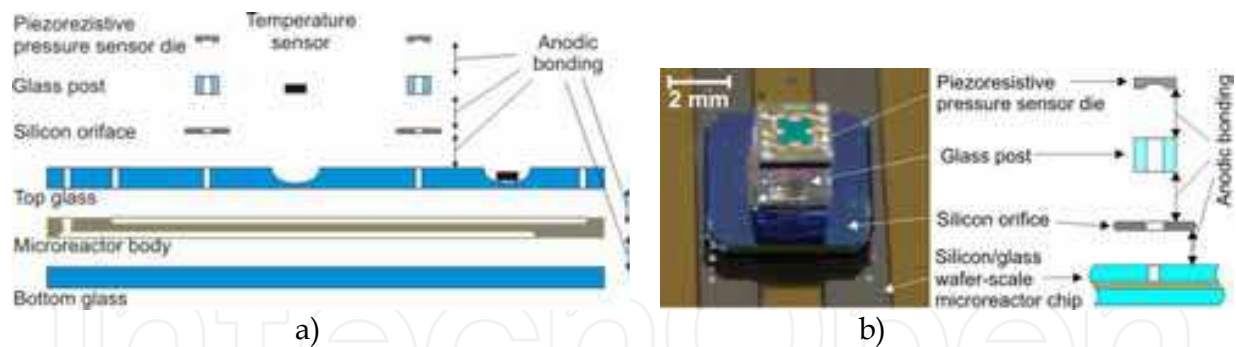


Fig. 7. The microreactor chip: a) cross-section of expanded view, b) details of the pressure sensor assembling

Packaging of the microreactor chip is an onerous but crucial problem. Package should fulfil following requirements: mechanically stable fixing of the microreactor chip, protection of the chip and sensors, electrical connections of the sensors and fluidic connections of channels.

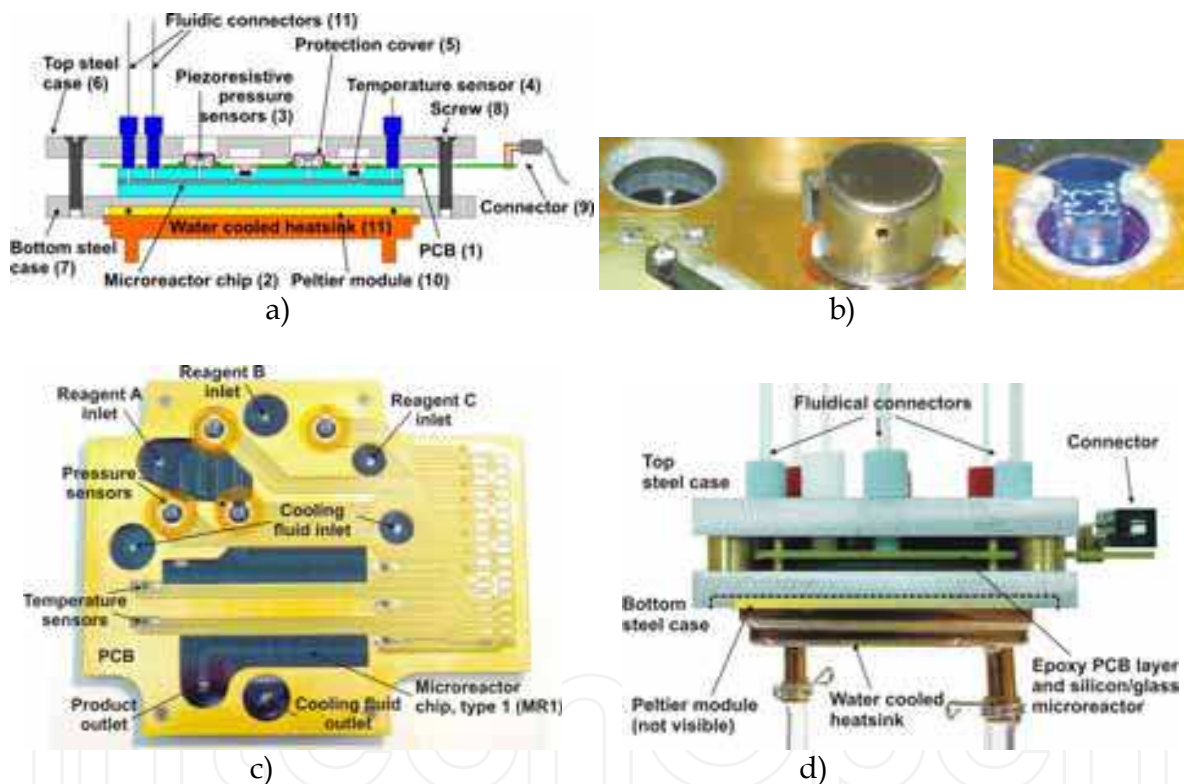


Fig. 8. The microreactor in a package: a) cross-section view, b) details of sensors assembling, c) microreactor chip with PCB board, d) a side view

The cross-sectional view of the packaged microreactor is shown in Fig. 8a. The PCB board (1) with a net of electrical paths is fixed (epoxy glued) to the microreactor chip (2). Pressure sensor dies (3) protrude from PCB board (1), so the wire-bonded electrical connections between dies and PCB can be done. Electrical connections of temperature sensors (4) are soldered with PCB board (1). Each sensor is protected by the metallic cup (5) glued to the PCB board (1). The top (6) and the bottom (7) steel case is positioned and screwed on (8). Output electrical connections are provided by slide-type connector (9). The Peltier module (10) (TM-127-2.0-1.5, Transfer Multisort Electronic, Poland) with heat exchanger is fixed to the back-side of the bottom steel

case (7), to increase the cooling efficiency and to steer and/or control general temperature conditions inside the microreactor chip. The heat exchanger is made of water cooled heatsink (11) (CPC, Poland).. Teflon® fluidic connectors (12), are placed in the top case (6).

2.2.3 Miniature, discreet, corrosion-resistant pressure sensor

Independent from the microreactor, corrosion resistant and ultra-low “dead” volume pressure sensor enabling measurement of the pressure inside microreactors made of ceramic, polymers and metal, were strongly required. The new concept of the discrete pressure sensor is based onto an “inverted” principle of packaging and protection of the micromachined silicon pressure sensors die (Fig. 9a). In commonly known designs of corrosion resistive pressure sensors, the die is placed inside a metal case and is protected by a metal separation membrane welded to this case. Inner chamber of the sensor is fulfilled with an oil, working as a hydraulic pressure medium between external environment and thin membrane of the die. Such construction is characterized by the large dead volume, ranging several millilitres, what cannot be tolerated if sensors are applied in the microreactor which dead volume is smaller. The new principle inverses the situation. The metal case is “suspended” on a silicon/glass die, measured media deflects membrane of the die upward. In this solution, there is no need of using of the additional separating metal membrane, dead volume of the sensor is equal to several microlitres and the only wetted surfaces of the sensor are made of corrosion resistant glass and silicon.

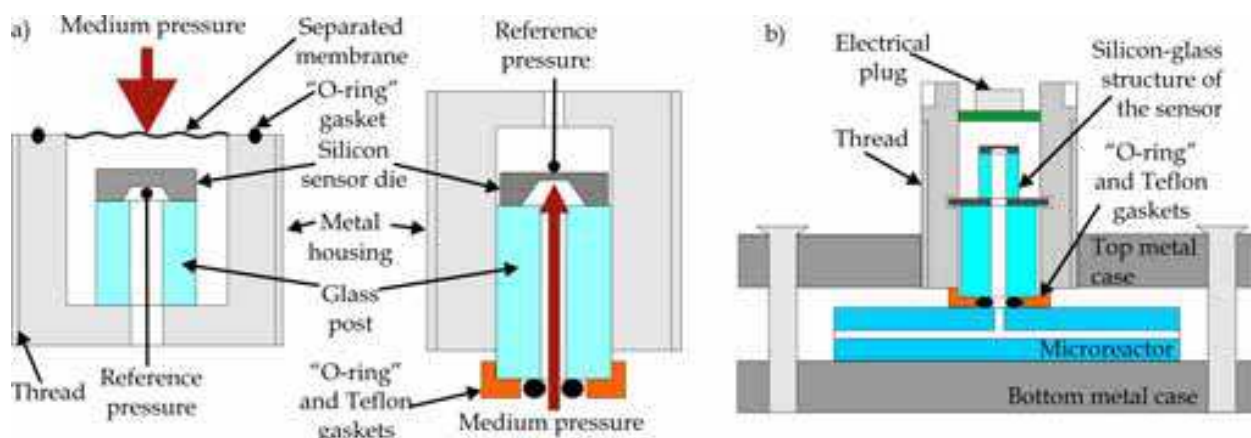


Fig. 9. Principle of the construction of the discrete pressure sensor: a) comparison of typical and novel construction, b) principle of sensor integration with the microreactor

The standard silicon-on-glass pressure sensor chip (silicon die bonded anodically to glass post, ITE Warsaw, Poland) were used. The pressure sensor chip is assembled to a silicon orifice and special glass post afterwards. Assembling was done by the use of the anodic bonding process. The complete multilayer silicon-glass structure is glued into a metal housing with outer thread. Special construction of the metal housing allows to screw the sensor in the top housing plate of the microreactor. Principle of the fluidic connection formation between pressure sensor and microreactor is shown in Fig. 9b. The sensor is screwed into the top metal case, specially designed Teflon® orifice in tandem with Viton® “O - ring” orifice ensure tight fluidic connection between the pressure sensor and the microreactor.

The miniature pressure sensor is chemically robust against concentrated and hot acids (except HF). The distinguishing feature is extremely low dead volume - about 8.5 μl for

single sensor. Total dead volume of fixed sensor, including capacity of via-hole made in microreactor connecting the sensor and microfluidical channel, is 9.2 μl .

Metrological parameters, chemical robustness against acids and tightness of set of gaskets of the new pressure sensors were tested. Electro - pneumatic tests have indicated, that the total error of the new sensors is below 1 % for fixed temperature. The temperature sensitivity coefficient, equal to 0.3 %, is significantly higher than noticed for the unpackaged dies (Table 4).

Normal work ratings:

| Parameter | Value | Unit |
|----------------------------|-------|--------------------|
| Nominal pressure | 600 | kPa |
| Overload pressure max. | 750 | kPa |
| Current supply typ. | 1,0 | mA |
| Current supply max. | 1,5 | mA |
| Voltage supply typ. | 5,0 | V |
| Voltage supply max. | 7,5 | V |
| Operating temperature max. | 50 | $^{\circ}\text{C}$ |
| Operating temperature min. | -10 | $^{\circ}\text{C}$ |
| Storage temperature max. | 85 | $^{\circ}\text{C}$ |
| Storage temperature min. | -10 | $^{\circ}\text{C}$ |

Metrological parameters:

| Parameter | Value | Unit |
|--|-------|-----------------------|
| Full scale output voltage (FSO) * | 56,1 | mV/V |
| Offset voltage* | 25,5 | mV |
| Bridge resistance * | 5 | k Ω |
| Non-linearity * | 0,38 | % |
| Pressure hysteresis * | 0,33 | % |
| Sensitivity coefficient * | 9,7 | mV/V/100kPa |
| Temperature offset coefficient ** | 0,1 | %/ $^{\circ}\text{C}$ |
| Temperature sensitivity coefficient ** | 0,32 | %/ $^{\circ}\text{C}$ |
| Total error * | 0,85 | % |

* at 25 $^{\circ}\text{C}$, $I_{\text{supply}}=1,0$ mA, $I_{\text{max}}600$ kPa

** average value over temperature range 0 $^{\circ}\text{C}$ to 50 $^{\circ}\text{C}$

Table 4. Basic parameters of discreet pressure sensor

Time-dependent characteristics of the new pressure sensor and reference sensor (Festo, SDE1 series, 600 kPa range) are similar. Chemical resistance of the pressure sensors have been investigated by 100 hours-long test with the use of concentrated sulphuric and nitric acids at ambient temperature and at 60 $^{\circ}\text{C}$. No influence on sensors parameters, leakages, corrosion effects have not been noticed. Leak-tightness of the fluidic connection is excellent. No leaks were observed up to 850 kPa.

2.2.4 Foturan®-glass microreactor equipped with discrete sensors

The developed discreet pressure sensor has been worked in tandem with a Foturan®-glass microreactor (Dietrich at al., 1996; Freitag at al., 2001). The microreactor consists of 12 layers which are photo-structurized in separate processes and following, all of them are bonded together in a fusion bonding process.

Cross-sectional view of the assembled microreactor with sensors is shown in Fig. 10, true pictures of parts and ready-to-work microreactor are shown in Fig. 11 and 12.

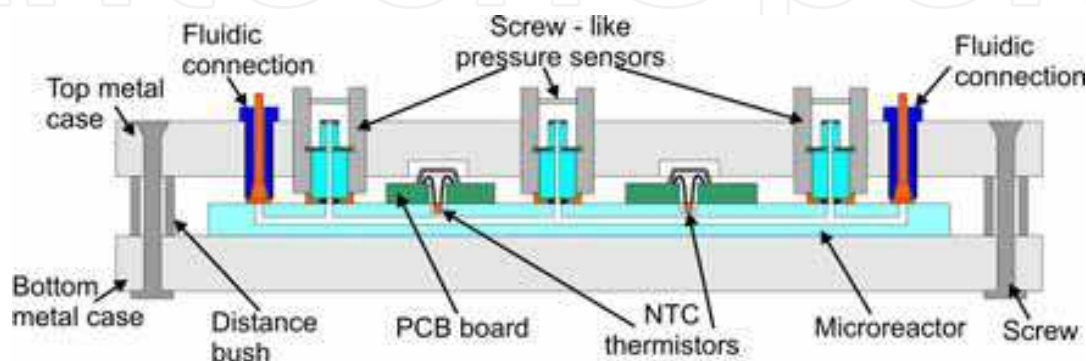


Fig. 10. Cross-sectional view of the packaged microreactor with set of sensors

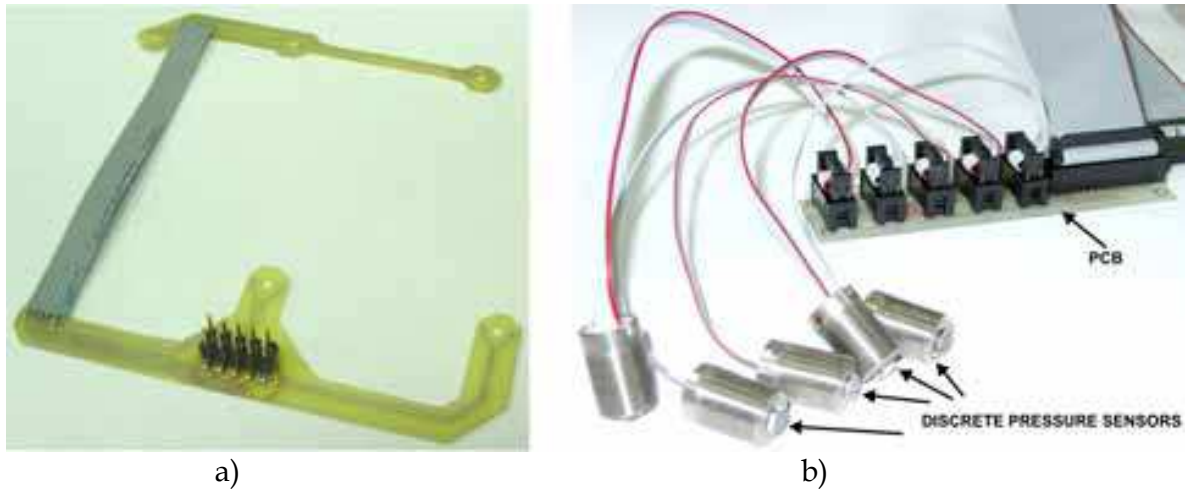


Fig. 11. The PCB boards, a) first PCB board with fixed temperature sensors, b) second PCB board for electrical signals collection from five screwed pressure sensors

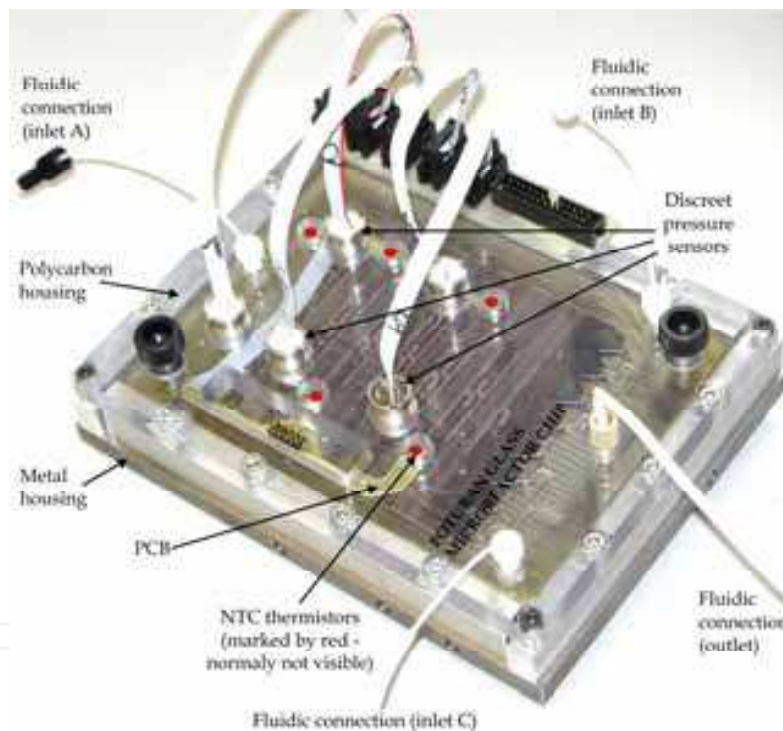


Fig. 12. Foturan®-glass microreactor equipped with 5 discrete pressure sensors and 5 temperature sensors (NTC thermistors)

Foturan® microreactor (Mikroglass GmbH, Mainz, Germany) was positioned between two plates of the case. In the laboratorial version of this package, top plate was made of light transparent carbonate. Pressure sensors were screwed, as described before. Temperature sensors (NTC thermistors, the same as described earlier for silicon/glass microreactor) were placed inside blind-holes made onto the top layer of the microreactor, in a close contact to the fluidic medium flowing inside microchannels and electrically connected, by soldering, to the PCB board with a electrical plug. Standard fluidic connections were screwed. Pressure sensors and fluidic connectors pressed microreactor downward, stabilizing it inside the case.

2.3 Pressure and temperature monitoring systems

No commercial, ready-to-use measurement systems, suitable to previously described sensors, have been available. It extorted to work out electronic/software system from the ground up. Laboratorial and commercial-like monitoring systems, based on data-acquisition card and self designed electronics and software, respectively, have been developed.

The system consist of to main parts: analogue and digital software parts plus software platform. Analogue part is supplying sensors and amplifying signal from sensors to voltage/current signal of useful range (0-3.3 VCD or 0-5 VDC for microcontroller based electronics, 0-10 VDC or 4-20 mA for automation). Moreover, offset correction of pressure sensors output signal is desired. Second, digital (software) part must proceed previously digitalized data, visualized them on graphs (bar-graphs, time-graphs, etc.) in desired units. Nevertheless, data recording is also required.

The block-diagram of the analogue part, driving several pressure and temperature sensors, is shown on Fig. 13.

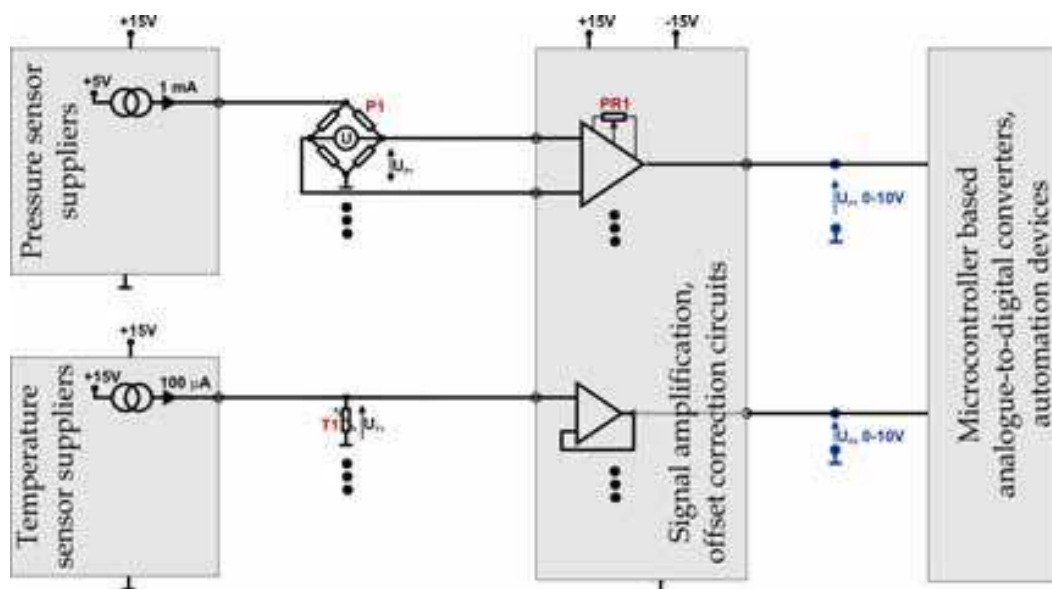


Fig. 13. Block-diagram of the analogue part of the monitoring system

Piezoresistors of pressure sensor are set to the Wheatstone bridge configuration. It is beneficial to supply one diagonal of the Wheatstone bridge by constant, stabilized current of 1.0 mA. Non equilibrium voltage, related to the measured pressure, is collected on the second diagonal of the Wheatstone bridge. Following, corrected (offset) and amplified voltage signal is digitalized.

Constant current supplying of the temperature sensors has been proposed as well. Temperature sensors, especially miniature sensors, must be supplied by low current. High value of supplied current will indicate self-heating of the temperature sensor, what in consequence will change resistance and true temperature can not be measured. Optimal value of supplying current (100 μ A) has been found.

The laboratorial version of the measurement system, consists of three PCB boards (PCB of pressure sensors suppliers 5 \times 1.0 mA, PCB of temperature sensors suppliers 5 \times 100 μ A and PCB of instrumentation amplifiers for correction and amplifying signals), data acquisition card (National Instruments). Processed signals are transfer through USB standard from data

acquisition card to a PC computer equipped with LabView-based software, where final signals processing, data visualization and data recording are done.

The laboratorial system has been combined with previously described glass-silicon-glass microreactor. The microreactor equipped with 4 pressure sensors and 5 temperature sensors, has been electrically connected to the measurement system. Following, static and dynamic fluidic tests were done. Tests have shown very good work of the system. Probably for the first time ever, true value of the pressure and its changes in time have been measured inside microchannels of the microreactors. System indicated precisely any of pressure instabilities caused by improper work of external pumps or gas bubbles inside channels, as well as blow-up of the microreactor intentionally caused by uncontrolled increase of the inlet pressure (Fig. 14). Temperature and its variation in time has been very precisely measured, the no cooling / cooling effect has been identified as well (Fig. 15).

Commercial-like measurement system, based on the same as previous one block-scheme, has been developed (Knapkiewicz at al., 2008). The electronic part of the system consists of analogue part (sensors supplying, signals amplifying) and self-designed data acquisition card. The system shown on Fig. 16, allows to connect and processed data from 5 of 2nd generation miniature, discreet pressure sensors (Fig. 17). Signals of sensors are pre-processed and sent to the PC computer equipped with specialized software with functions of data processing, presentation and recording. The “electronics” use USB connection for data transfer. Additionally, the system is equipped with analogue outputs useful for any kind of data acquisition systems. The quantity of channels for pressure sensors can be easy enlarge, temperature sensors channels can be added as well.

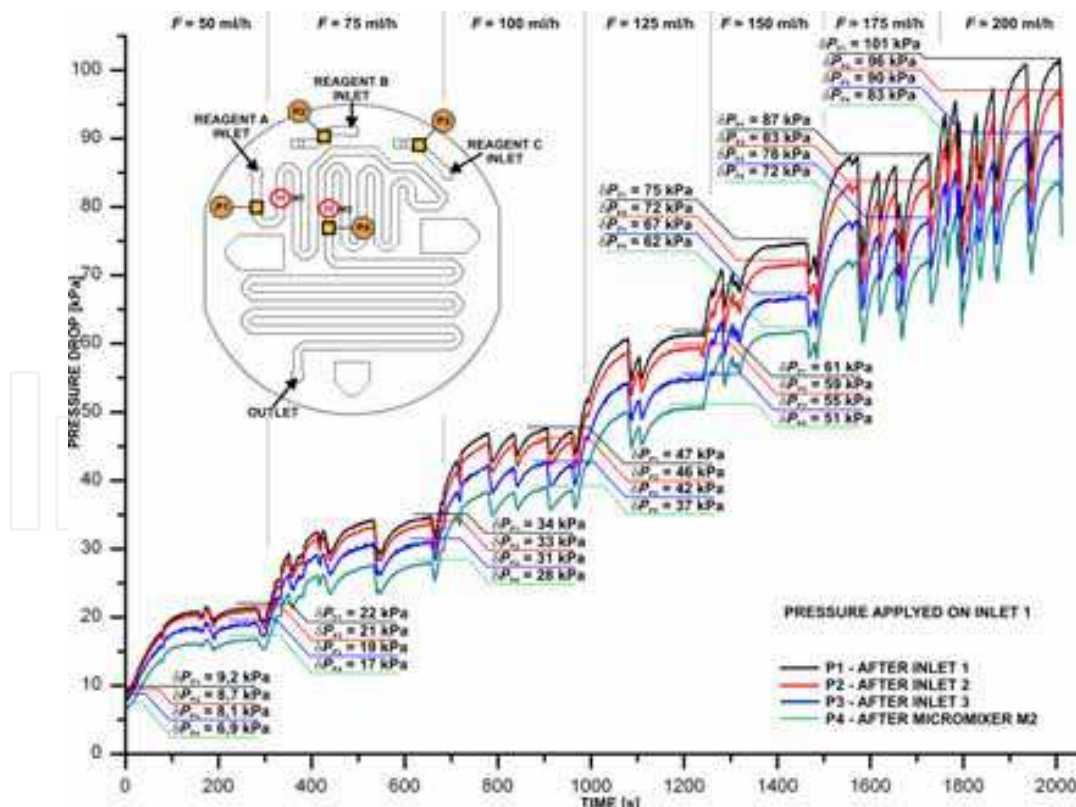


Fig. 14. Pressure drop for different flows of DI water as measured by developed pressure sensors, please note clear detection of pressure instabilities caused by irregular work of the dosing pumps

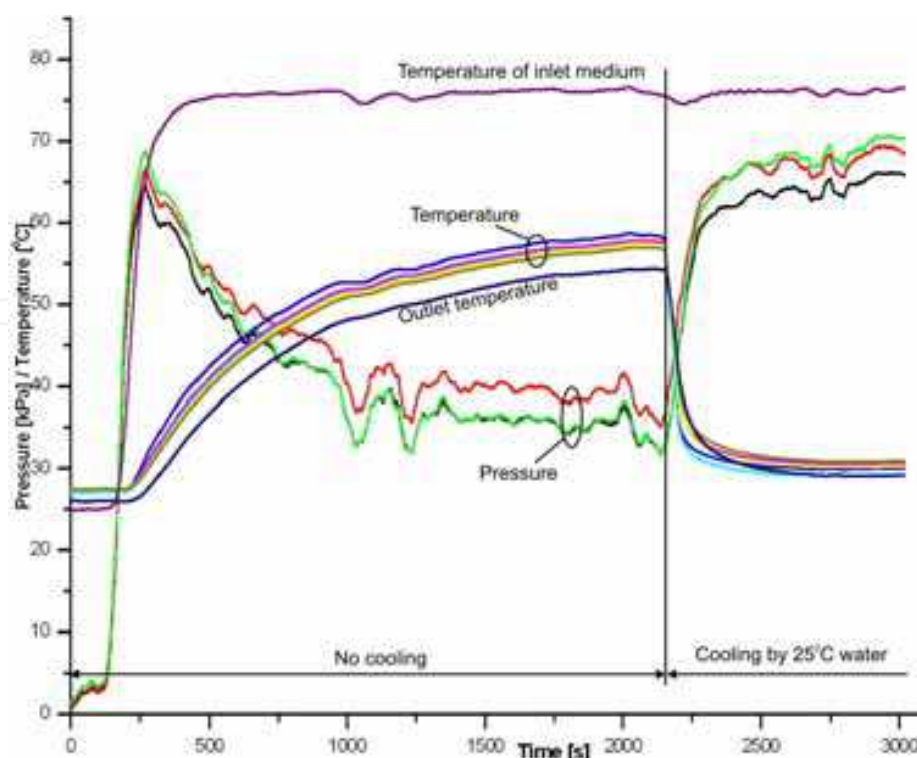


Fig. 15. Pressure and temperature time-related curves as measured by 5 temperature sensors and 4 pressure sensors, please note temperature decreasing while cooling was applied



Fig. 16. Commercial-like measurement system driving 5 discrete pressure sensors

The new, discrete pressure sensor and measurements system were used to build the "intelligent" microreactor, which was used as a key component in a "desk-top" microchemical plant for nitration processes. The "intelligent" microreactor consists of the previously presented Foturan® glass microreactor. Nitration of fluortoluene was conducted in the "desk-top" microchemical plant with simultaneous recording of information about pressure and temperature in insight microchannels.

The recorded data were presented as time-dependent curves where crucial points of the process, such as the start of flow, initiation of nitration, as well as drastic fluctuations of pressure for high values of reagents flow and corresponding to those fluctuations of temperature involved by pumps (switching of syringe pumps) were observed. Dramatic increases of temperature at the outlet of

the microreactor being an effect of destabilization of nitration reaction was properly detected. Examples of multi-parametrical measurements of reaction course are shown in Fig. 18.

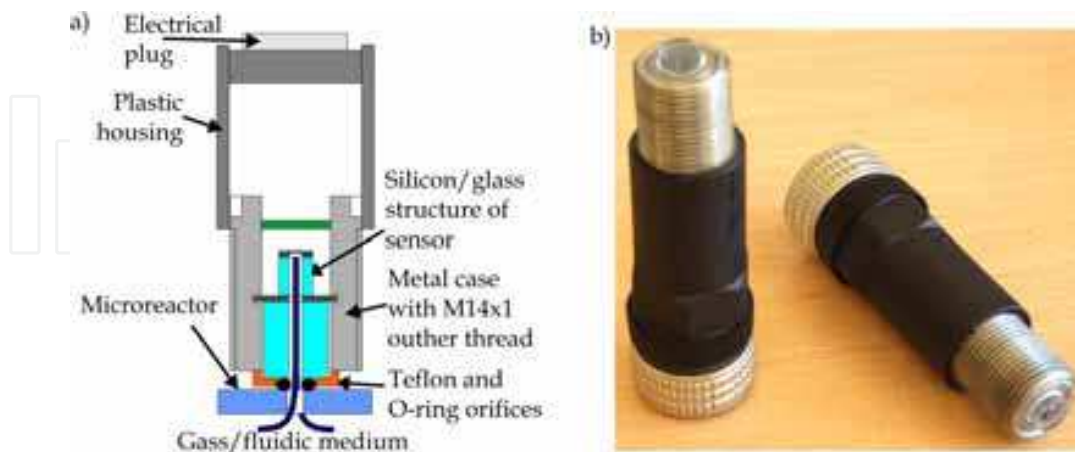


Fig. 17. 2nd generation of discrete pressure sensor: a) cross-sectional view, b) sensors ready to work

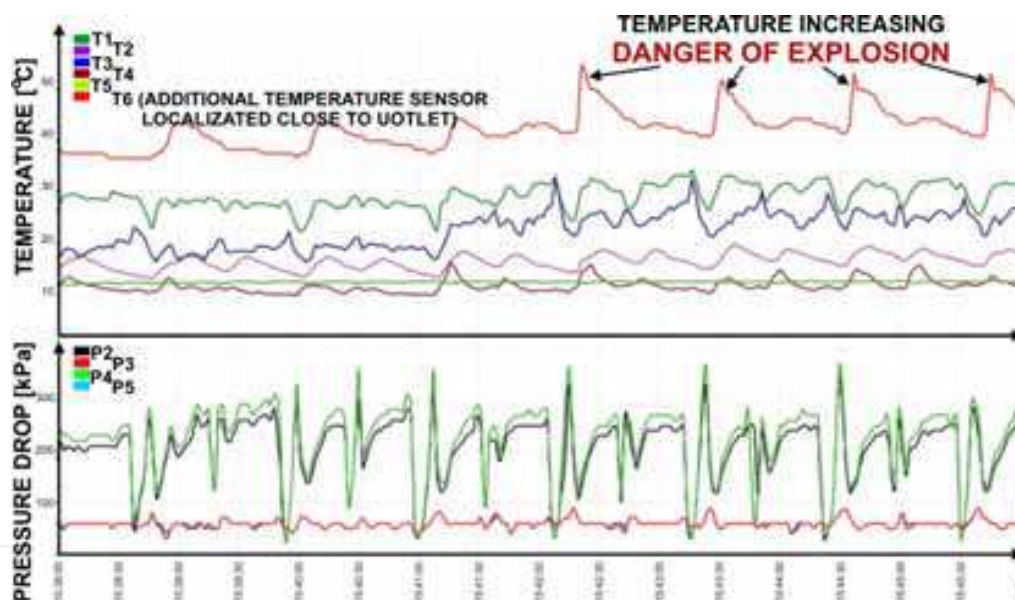


Fig. 18. Pressure and temperature versus time, nitration of fluorotoluene, total flow $F = 23,2$ ml/min)

2.4 Conductmetric, flow-through detector

Conductometric detection is widely applied in analytical chemistry what led to wide application of this technique in microfluidical analytical device often called also lab-on-a-chip. This technique utilizes dependency of electrical conductivity on concentration of ions in analyzed sample. It is commonly applied as detection technique in dielectrophoretic separation of organic and nonorganic compounds. Conductometry can be performed in two basic modes: contact and contactless. Various materials can be utilized as the chip body (silicon, glass, polymers, ceramic) but electrodes are usually made of gold, platinum or chromium. The main problem occurring in contact mode of conductometric measurement is

possibility of electrochemical reaction observed on the surface of the electrodes. Therefore, technical realizations of contactless mode is developed rapidly. It eliminates reactivity with analyte and enables better electrical isolation of the electrodes in relation to the potential utilized in dielectrophoretic separation of the analyte.

In this subchapter we present an example of discrete silicon-glass microfluidical contact conductometer with various configurations of electrodes. Then, an integrated microdoser with built-in two-electrodes conductivity detector to monitor on-chip volume of dosed analyte is presented.

2.4.1 Discrete microfluidical flow-through conductometric detector

The conductivity microdetector is a silicon-glass structure with galvanic feedback of three metallic electrodes (Fig. 19).

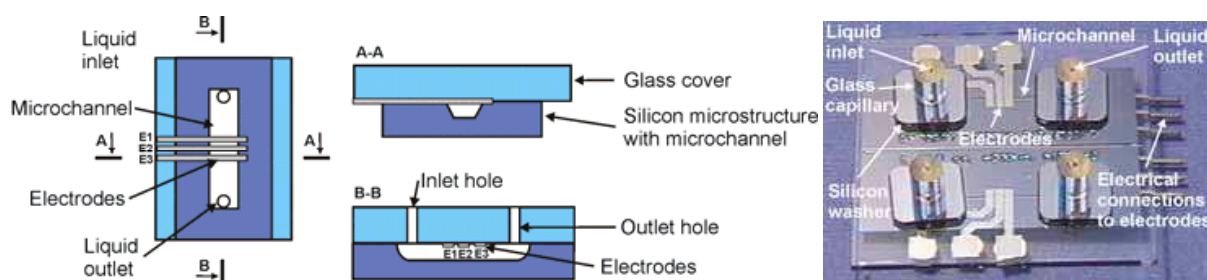


Fig. 19. The conductivity microdetector: a) schematic views of the detector, b) assembled device with double detector structure and the silicon-glass fluidical connections

The silicon body ($35 \times 35 \text{ mm}^2$) of the microdetector was fabricated on the (100)-oriented, one-side polished, n-type, $5 \Omega\text{cm}$ wafer. The microchannel (18 mm long, $300 \mu\text{m}$ width and $140 \mu\text{m}$ deep) was anisotropically etched in 40% KOH at 80°C through thermal silicon dioxide ($0.5 \mu\text{m}$ thick) mask layer. Then, SiO_2 was removed in BHF and the wafer was once again thermally oxidized ($0.3 \mu\text{m}$ SiO_2) to form chemically resistance layer. The glass cover of the microdetector was made of the 1.1 mm thick Borofloat 3.3 substrate. Three metallic electrodes, designed as $1000\text{-}\mu\text{m}$ -width strips, were formed on the selected surface of the glass substrate with different distance between them - $75 \mu\text{m}$ between E1 and E2 and $120 \mu\text{m}$ between E2 and E3. The electrodes were made of sputtered Cr/Ni/Au (100/50/150 nm) multilayer. The dead volumes between E1 - E2, E2 - E3 and E1 - E3 electrodes were 87 nl, 89 nl and 135 nl respectively. The input/output holes ($\phi=0.9 \text{ mm}$) for the liquid were mechanically drilled in the substrate. The silicon die and glass cover were washed, hydrofilized and anodically bonded (2 kV, 450°C). In order to minimize the dead volumes of the connections the special silicon-glass connections were applied. The glass capillaries were anodically bonded (1.5 kV, 450°C) through the silicon washers to the microdetector chip. The steel capillaries were glued to the inlet holes of the glass capillaries.

The static characteristics of microdetector were measured at a specially designed test station (Fig. 20). The syringe pump (Prefusor, Germany) ensured constant, pulsation free liquid flow (1.2 ml/h). The microdetector was supplied by sinusoidal-wave generator with constant (0.4 V) amplitude. In the two-electrodes configuration the output voltage was measured at $100 \text{ k}\Omega$ series loaded resistor by Metex M4650CR (Metex Instruments, Korea) and collected by PC under ScopeView software. In the three-electrodes set up, the outer electrodes (E1, E3) were supplied by the sinusoidal signal and the output signal was collected from the middle electrode (E2).

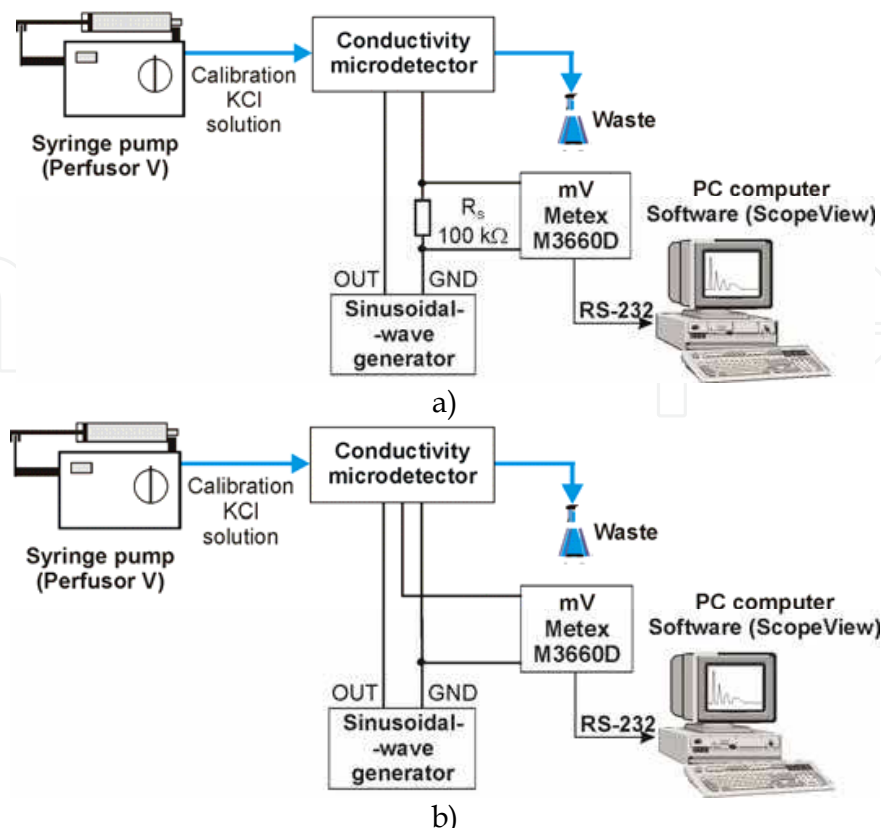


Fig. 20. Schemes of the measurement stations for conductivity microdetector characterization in: a) the two-electrodes configuration, b) the three-electrodes configuration

Tests of the conductivity microdetector were carried out to find the optimal configuration of the electrodes and supplying signal frequency (f_{SUPPLY}). The output signal and sensitivity of the microdetector, defined as change of the output voltage (in mV) in relation to change of the molar concentration of the calibration solution (in mM), have been determined. The highest output signal of the microdetector, for $f_{\text{SUPPLY}}=1$ kHz, was obtained for concentrated KCl solutions and three-electrodes configuration (Fig. 21a). In the range of the low concentrated KCl (0.5 mM ÷ 10 mM) the sensitivity of the microdetector (S_1) was also the highest ($S_1=8.38$ mV/mM) for three-electrodes configuration. The E1 - E2 configuration had slightly lower sensitivity ($S_1=8.28$ mV/mM). The E2 - E3 set up had about 60% lower sensitivity than the previous configurations. In the range of more concentrated KCl (10 mM ÷ 100 mM), the highest sensitivity (S_2) was observed for E1 - E2 configuration ($S_2=0.4$ mV/mM), the lowest - for three-electrodes system ($S_2=0.15$ mV/mM). It has been concluded, that the two-electrodes configuration (E1 - E2) was the optimal, from the point of view of the micro dosing device, set up of the electrodes. For two-electrodes configuration, the output signal of the microdetector was the highest for above 4 kHz supplying signal frequency and concentrated KCl (Fig. 21b). However, the highest sensitivity ($S_1=8.28$ mV/mM and $S_2=0.4$ mV/mM) was observed for $f_{\text{SUPPLY}}=1$ kHz (Fig. 21c). The lowest detection limit was estimated to be about 0.01 μl for 1 mM KCl.

Obtained results were close to the known from the literature typical values of the supplying signal for the conductivity measurements with galvanic feedback (Zemann, 2001). These values ensured high sensitivity of the microdetector in the wide range of the applied KCl

solution concentrations and low, but easily measurable output signal of the microdetector, advantage from the point of view of the life-time of the thin electrodes. It will be also advantage to decrease the distance between electrodes to increase the microdetector sensitivity for the low concentrated KCl solutions.

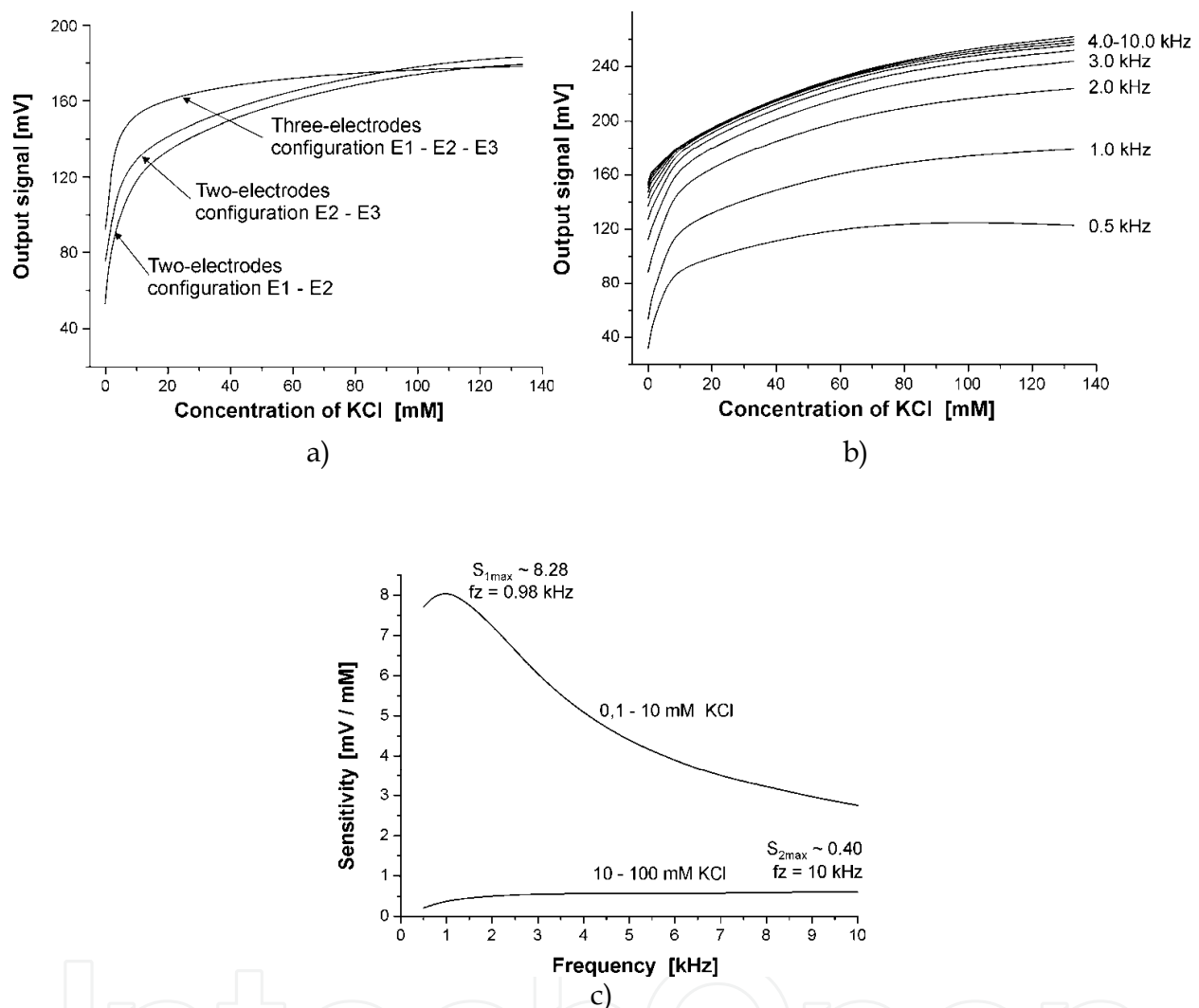


Fig. 21. Conductivity measurements: a) the output signal of the microdetector for different electrodes configuration as a function of the KCl solution concentration, supplying sinusoidal signal with 0.4 V amplitude and 1 kHz frequency, b) the output signal of the microdetector in E1 - E2 electrodes configuration as a function of the KCl solution concentration for different frequency of the supplying sinusoidal signal with 0.4 V amplitude, c) sensitivity of the microdetector in E1 - E2 electrodes configuration as a function of the frequency of the supplying sinusoidal signal with 0.4 V amplitude for different KCl solution concentration, fluids flow 1.2 ml/h

3.4.2 Microdoser with integrated conductometric detector

An idea of a micro dosing device with the pressure driven injection of analyte and on-chip monitoring of the dosed volume is schematically presented on Fig. 22. The on-chip monitoring of the injected volume is ensured by a conductivity microdetector positioned near the outlet.

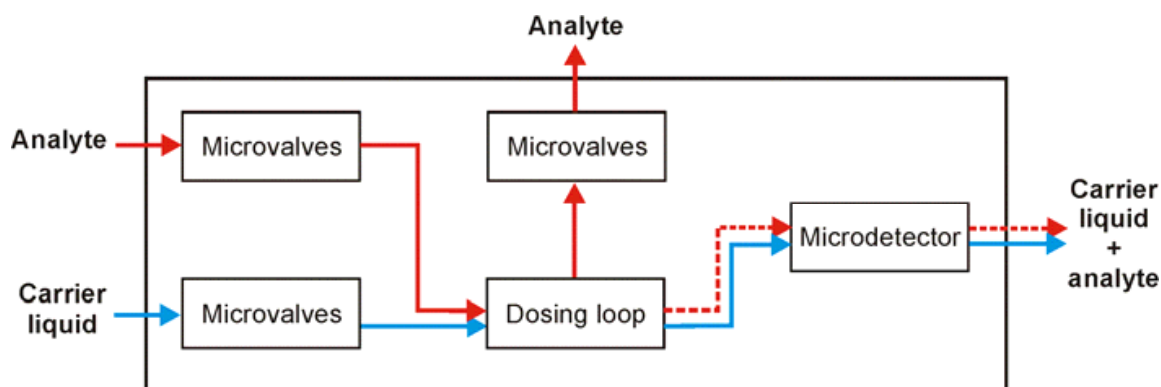


Fig. 22. Scheme of the integrated dosing device with built-in conductometric detector

In a stand-by mode (Fig. 23a), microvalves MV2, MV3 and MV4 were closed while valves MV1, MV5 and MV6 remained open. A carrier liquid (buffer) flowed from inlet 1 to output 3, through the conductivity microdetector. The microdetector measured time-dependent conductivity of the flowing-through samples. The analyte flowed from inlet 5 to outlet 4 and fulfilled the dosing loop. At a dosing mode (Fig. 23b), microvalves MV1, MV5 and MV6 were closed while MV2, MV3 and MV4 were opened. The carrier liquid flowed through the dosing loop and flushed the sample to output 3. The loop was purified and the device was prepared to the next injection. Then, the net of microvalves was switched to the stand-by mode. The fixed maximal volume of the dosed analyte was equal to the volume of the dosing loop (700 nl). Smaller volumes could be dosed by controlling the time of the dosing mode by switching the proper set of microvalves.

Fabrication procedure of the dosing device with Kapton® film as the membrane material of the microvalves was based on microengineering techniques. Structures of the six microvalves and net of 200 μm -deep and 400 μm -wide microchannels were etched in a (100)-oriented n-type 5 Ωcm silicon wafer in 40% KOH at 80°C through thermally grown silicon dioxide (1 μm thick) mask. The after-etch SiO_2 was removed in BHF. Next, micromachined wafer was again thermally oxidized (0.3 μm) to obtain chemically resistance cover. Following, the steering chambers of microvalves (220 μm -deep) were isotropically etched in 40% HF at room temperature in 1.1 mm-thick Borofloat 3.3 through the mask made of the self-adhesive foil (Semiconductor Equipment Corp., USA). The inlet/outlet via-holes ($\phi = 0.9$ mm) for gas and fluids were drilled mechanically. Afterwards, two Cr/Ni/Au (50/50/200 nm) electrodes of the conductivity microdetector were deposited and patterned on the processed side of the glass substrate. The Cr/Au (50/150 nm) plates were formed on a chosen side of the Kapton® film to form anti-sticking layer. Next, the via-holes ($\phi = 0.9$ mm) were cut in the film. Wafers and film were washed in 30 % H_2O_2 at 80°C, rinsed in DI water and dried in the stream of pure N_2 .

The silicon wafer and glass cover, aligned to each other, were sealed under adhesive bonding at about 270°C through Kapton® film (Fig. 24). Fluidical connections were made of cut glass tubes with polished front surface, sealed by use of the UV curable UVO-114 epoxy-glue (EpoTec, Germany). Gas ports were made of medical needles ($\phi=1$ mm) glued to glass cover by epoxy-glue. Next, the dosing device was mounted onto PC board. Electrical connections between conductivity sensor and BNC ports were made by wire soldering.

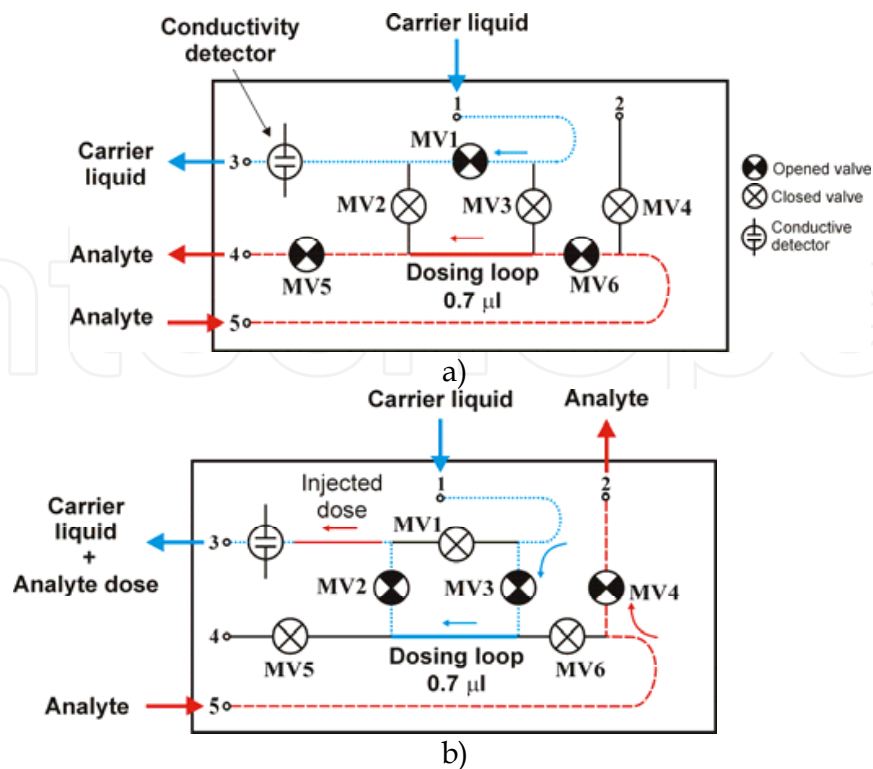


Fig. 23. The dosing device: a) the principle of working of the micro dosing device in the stand-by mode, b) in the dosing mode

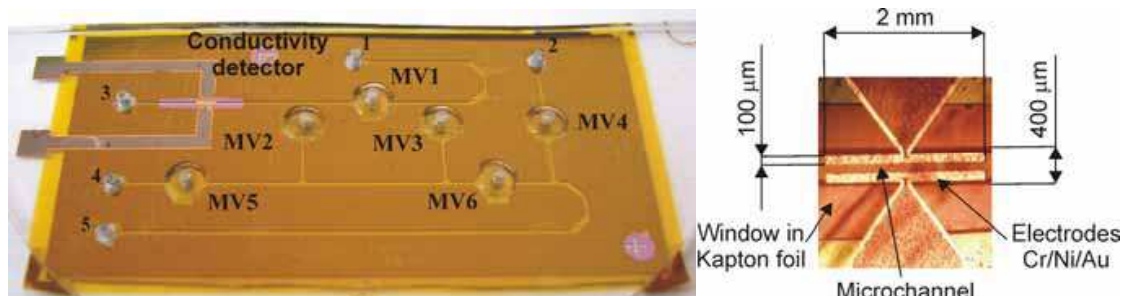


Fig. 24. View of the assembled doser chip (left picture) with enlarged area of conductometric detector (right picture)

The measurement set up for test of the micro dosing device (Fig. 25) contained pneumatic facilities: external electromagnetic valves (EV) (Festo, Germany), normally-open EV1 for MV1, MV5, MV6 and normally-close EV2 for MV2, MV3, MV4, steering pressure P_{STEER} regulator and nitrogen or air gas containers. Flow of the liquid carrier and analyte was ensured by double syringe pump (Perfusor, Germany). The conductivity microdetector was supplied by sinusoidal-wave generator. The output voltage was measured at 100 k Ω series loaded resistor by Metex M4650CR (Metex Instruments, Korea) and collected by PC under ScopeView software. The steering card DAS1402 (Keithley, USA) and LabView 6.0 (National Instruments, USA) software have been used for steering of the external electromagnetic valves. The dosing test were done for the 1 mM KCl injected into DI water. The flow of fluids was 1.2 ml/h. The conductivity detector was supplied with the previously determined optimal sinusoidal-wave signal parameters ($f_{\text{SUPPLY}}=1$ kHz, 0.4 V amplitude).

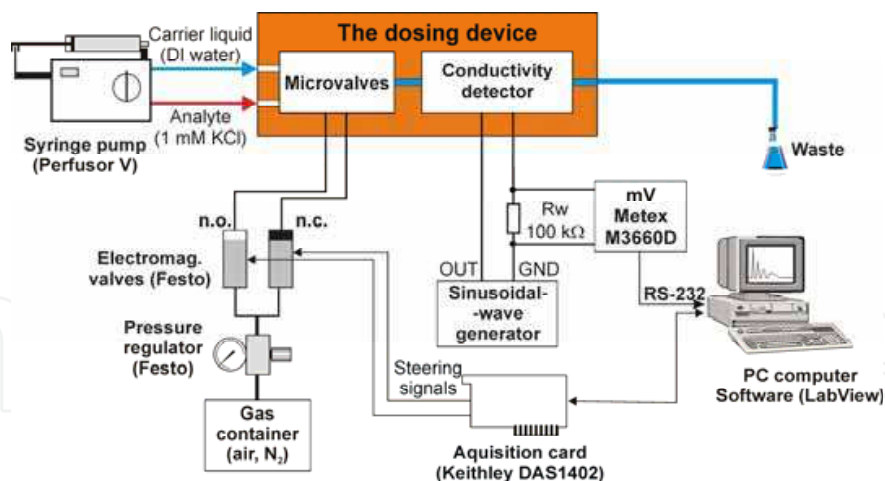


Fig. 25. The measurement set up for the tests of the doser

Thanks to the integrated conductometric detector it has been found, that the dose of the analyte may be adjusted in the range of 100 nl to 700 nl (Fig. 26a) by changing the opening time of the microvalves in the dosing mode. The precise dosing of the analyte with repeatability of the injected volume better than 4 % was obtained for 200 nl to 700 nl volumes. The injected volume had a variation of about 30 % for 100 nl dose. The dose-by-dose test have shown that the dosing device was able to dose the constant (600 nl) volume of the analyte in less that 50 seconds repetition time with the repeatability of the injected volume better than 2 %, what corresponded to 12 nl variation (Fig. 26b).

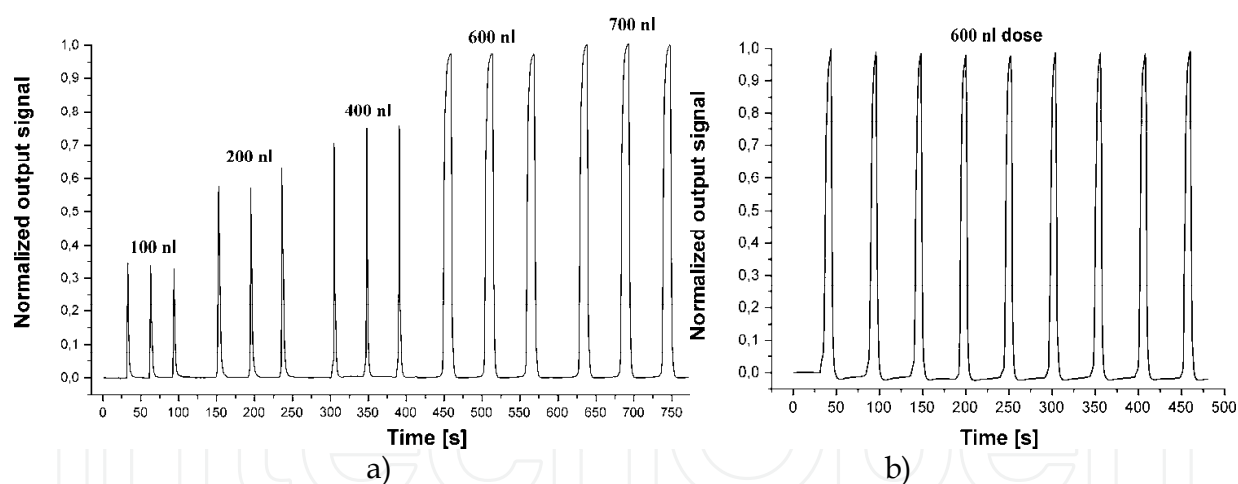


Fig. 26. Normalized output signal of the conductivity microdetector for: a) various dosing volumes of the analyte obtained by hydrodynamic injection of the volume of the dosing loop (700 nl) or adjusted by the time of the dosing mode (100 nl ÷ 600 nl), b) constant injected volume (600 nl) dosed in 50 seconds repetition time in the multiply-injection mode of the dosing device; dosed analyte: 1mM KCl, carrier: DI water, flow of fluids: 1.2 ml/h, conductivity microdetector supplying parameters: sinusoidal-wave, 1 kHz, 0.4 V

4. Optical microsensors

Among many detection techniques, optical sensing seems to be most widely used. It is because of well known methodology and instrumentation as well as high sensitivity and

contactless nature of the measurement. Two optical sensing methods are dominating in microreaction and lab-on-a-chip technologies - spectrophotometry and fluorometry. However, sensing problems arise while analyzed volume is decreased from millilitres to volumes characteristic for lab-on-a-chip techniques - nano- and picoliters. Therefore, usually high sensitivity detectors must be applied. There is a lot of examples of various technical realizations of different microfluidical chips dedicated for both optical methods. In case of spectrophotometry most of these examples are operating in visible light range (VIS), measuring optical properties of non-aggressive liquids (Bargiel et al., 2004). Here we present two unique examples of microfluidical transmittance microsensors for microreaction technique and lab-on-a-chip applications. While fluorometry is applied, typically bulky and expensive epifluorescence-like instrumentation co-working with microfluidical chip is utilized. Here we present a novel methodology and low-cost instrumentation enabling sensitive fluorescence detection induced in various types of labs-on-a-chip.

4.1 Transmittance NIR detector of chemically aggressive liquids

High heat and mass transfer rates in microscale allow the reactions to be performed at higher temperature, providing high yields that are not achievable in conventional reactors. However, real time analytical monitoring of the final product of reaction is necessary to suppress the unwanted by-products. Near-infrared spectroscopy (NIR) appears to be very useful for this purpose due to its capability of a real time, non-invasive monitoring of the chemical processes. The application of NIR spectroscopy in microreactor requires a suitable microsensor characterized by the very low dead-volume and high chemical resistance against for example hot, concentrated nitric and sulphuric acids. Typical spectrophotometric constructions of microfluidical detectors can not be applied in these aggressive conditions mainly due to lack of physical separation between measured liquids and optical fiber. The weakest point of these constructions is a method of optical fibers assembling, utilizing chemically non-resistive glues. It leads to rapid glue destruction and appearance of leakages what can not be accepted due to safety reasons. The unique feature of developed by us microsensor was application of thin silicon wall separating fluidic microchannel from microchannel with optical fibers. It is well known that thin (below 20 μm) silicon layer is transparent for near-infrared light (Fig. 27). Thus, physical separation with simultaneous NIR transmittance was obtained.

The technology of novel optical microsensor utilized standard microengineering techniques. The fluidic channel and alignment grooves were etched by deep reaction ion etching (DRIE) in 380 μm thick, double-side polished, (100)-oriented silicon substrate. DRIE process has been optimized to obtain the vertical side-walls of the channel. Two type of microchannels were formed. The first type was microfluidical channels, the second one - microchannels for positioning of optical fibers. After DRIE etching these two types of channels were separated by 20 μm thick silicon wall with perpendicular walls. Photolithographically patterned 100 nm Al mask layer was used to form fluidic inlet/outlet holes from back side of the wafer. The silicon substrate was thermally wet oxidized again to obtain 0.3 μm SiO_2 isolation layer serving as chemically resistive layer. Next, the silicon substrate was anodically bonded (450°C, 1.5 kV) to a Borofloat® 33 glass (Schott, Germany).

High quality bonding process was required to ensure the leakproofness of the channel. Finally, the optical fibers equipped with SMA connections were positioned in the alignment

grooves and immobilized by a droplet of UV-curable optical glue UVO-114 (Epo-Tec, Germany) (Fig. 28).

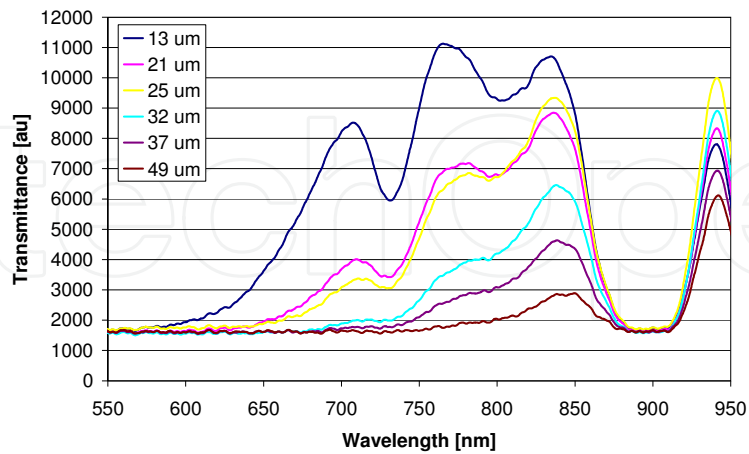


Fig. 27. Transmittance of thin silicon membrane (thickness from 13 μm to 49 μm)

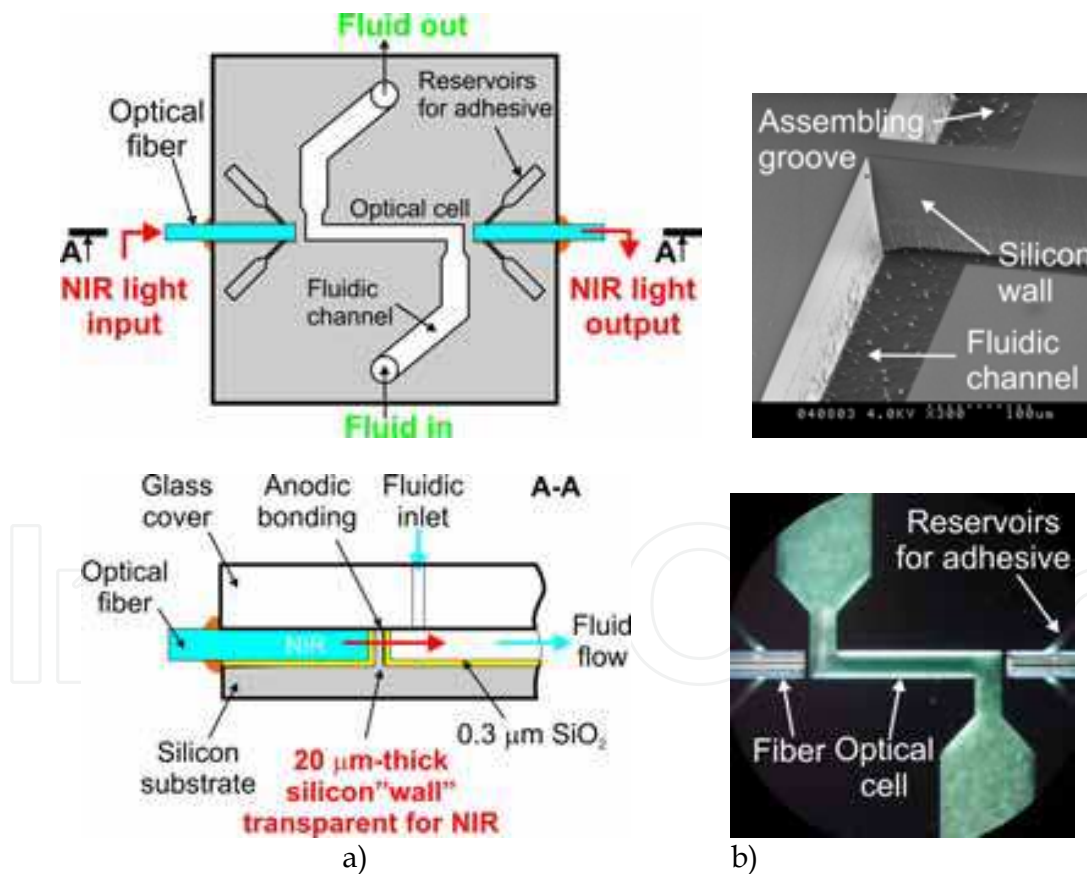


Fig. 28. NIR spectrophotometric microfluidical sensor: a) schematic top view and cross-section of the microsensors, b) SEM picture of the thin silicon wall separating microfluidical channels for liquids and optical fiber positioning after DRIE etching (upper picture) and optical microscope picture of the measurement cell with assembled optical fibers (lower picture).

Assembled microfluidical sensor was placed on a PCB carrier and mounted in a metal package with tight and chemically resistive standardized fluidic connections (UpChurch, USA) (Fig. 29a, b).

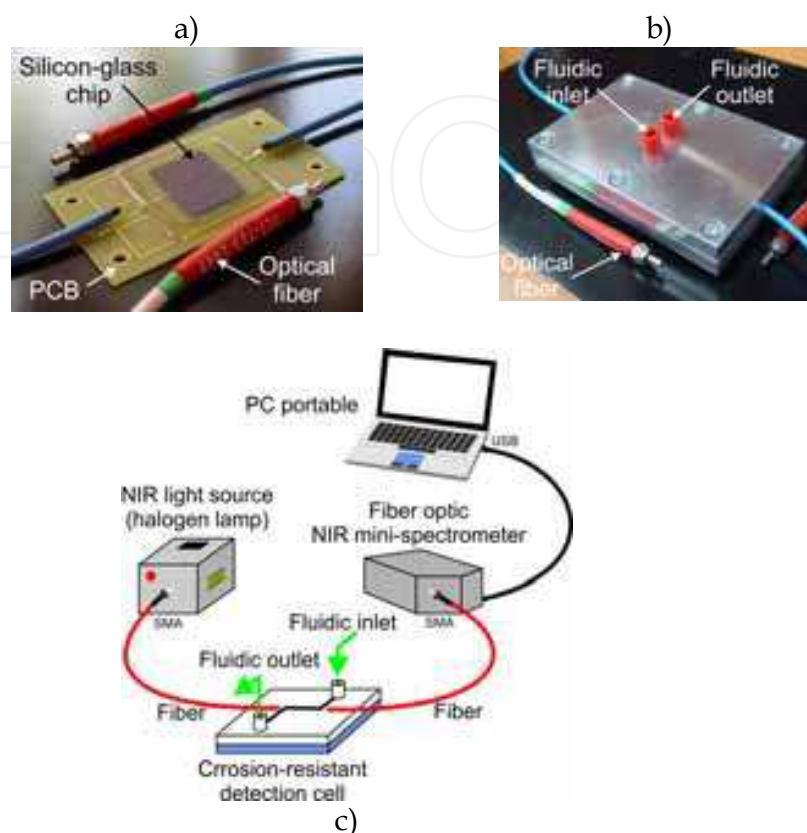


Fig. 29. NIR spectrophotometric microfluidical sensor: a) the chip mounted on a PCB ensuring proper mechanical stiffness and robustness, b) the chip mounted in a metal package ready with fluidic connections, c) scheme of the measurement set-up for NIR spectrophotometric characterization of aggressive liquids by microfluidical silicon-glass sensor

The NIR system was composed of a halogen light source, a silicon-glass corrosion resistant optical cell, and a NIR mini-spectrometer C9406 (Hamamatsu, Japan) (Fig. 29c). The cell with optical path length of 5 mm had detection volume of only 90 nL. The system was controlled by a notebook with suitable software.

The miniature spectrometric system has been tested experimentally by the measuring of NIR spectra of several samples including highly corrosive reactants of nitration reaction. The detection unit worked correctly at wide range of flow rates (0-300 ml/h) what confirmed its mechanical robustness. The 24 h-long test with the measurement cell filled with pure nitric acid followed by sulphuric acid showed corrosion resistance of the detection chip. The spectra of pure nitric and sulphuric acids as well as theirs mixtures with deionized water were successfully obtained (Fig. 30).

In further tests it has been clearly shown that the microsensors recognizes properly different diesel oils and furnace oil as well as gasoline. Concentration of ETOH in Porto red wine has been very well examined. Experimental results confirm the full applicability of the miniature corrosion resistant NIR spectrometric system for use in wide range of applications, e.g. mTAS, microreaction technology, biomedical/medical measurements. The

maximal wavelength is limited by the properties of array detector applied in miniature Hamamatsu spectrometer. The use of longer NIR wavelengths (up to 2500 nm) is not limited by the micromachined detection cell.

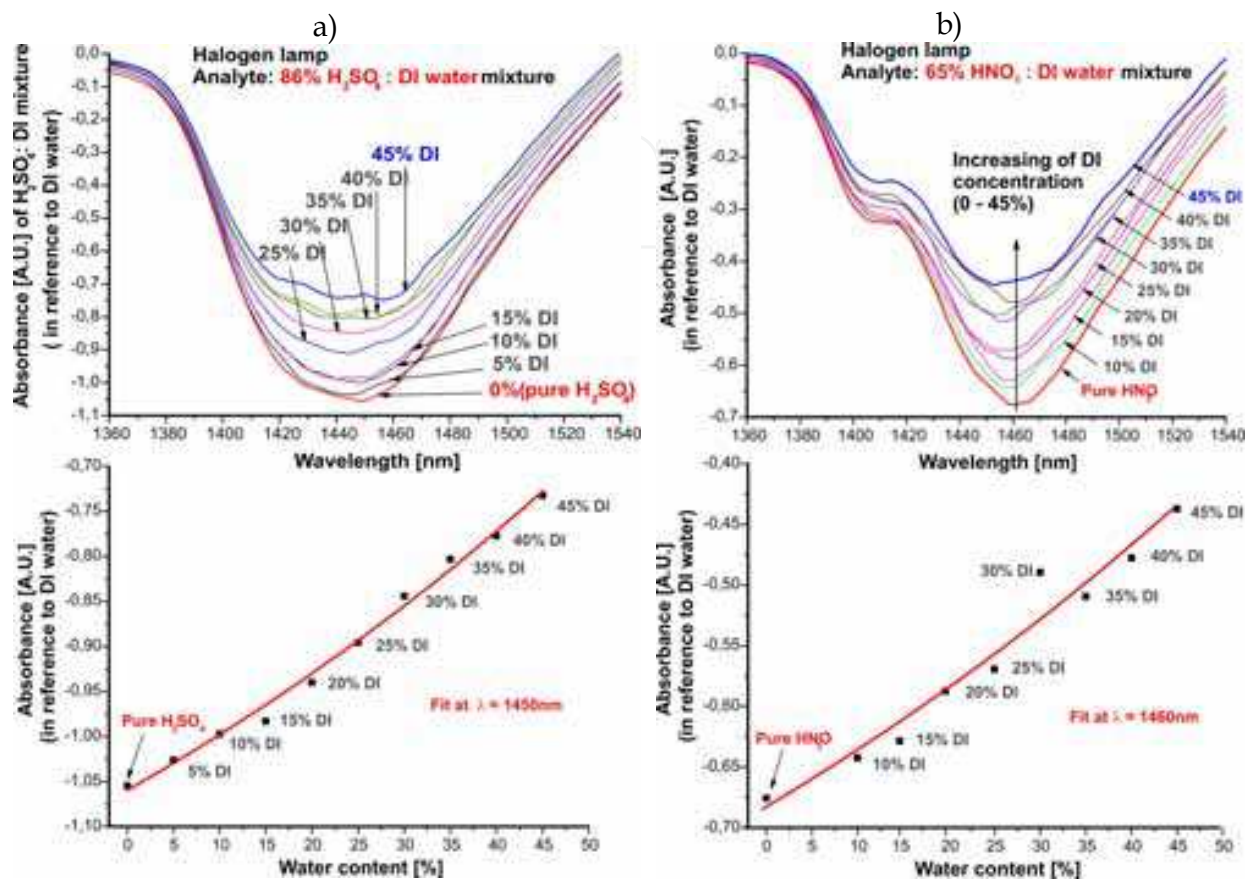


Fig. 30. The spectra of concentrated pure sulphuric (a) and nitric (b) acids as well as their mixtures with deionized water, calibration curves describing absorbance versus DI water content are shown below spectra

4.2 Absorbance VIS detector for optical characterization of living oocytes and embryos

Optical characterization of living reproductive cells is an important issue in assisted reproduction techniques. The major goal of these techniques is improvement of in vitro fertilization process towards more successful breeding of farm animals. It is well known that only 5-10% of in vitro fertilized oocytes are viable enough to reach full development competence embryo stage. Assessment of development competence of oocytes and embryos based on lab-on-a-chip system with analyze of the spectral characteristic of the cells, is an important element in research on assisted reproductive technologies. Typical diameter of porcine or bovine oocytes is in 100 μm - 150 μm range, similar dimensions are characteristic for embryos. Due to size and volume incompatibility, spectrophotometric characterization of these cells is impossible in typical measurement cuvette with 10 mm-long optical path and at least a few hundreds microlitres volume. On the other hand, miniaturized spectrometers and light sources co-working with optical fibers as light guiders to and from characterized object are available now. What more, lab-on-a-chip techniques enables

fabrication of microchannels with diameter similar to the size of oocytes/embryos and optical fibres (Szczepanska et al., 2009) (Fig. 31a).

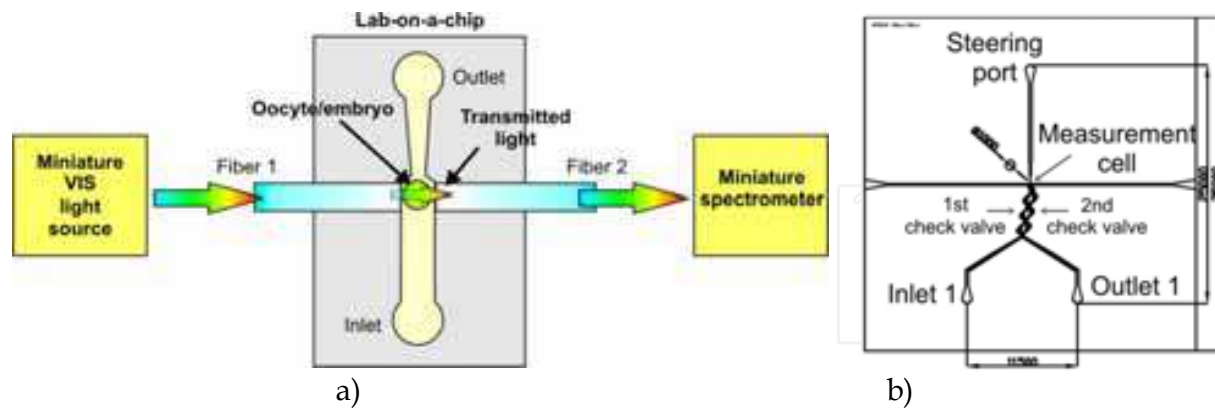


Fig. 31. Scheme of an idea of the spectrophotometric characterization of single oocyte or embryo in a lab-on-a-chip (a) and layout of the real lab-on-a-chip, the dimensions are in μm

Lab-on-a-chip contains measurement cell, net of microchannels and passive valves for steering of fluid and oocyte/embryo flow, and inlet/outlet holes for biological material loading/unloading as well as a steering port for fluid flow management (Fig. 31b). The biological material is introduced into the measurement cell by inlet 1, then passes through set of passive Tesla's valves (1st check valve). Next, characterized cell flows into the measurement cell by sucking of the fluid by a pipette connected to the steering port of the chip. Topology of the measurement cell ensures mechanical immobilization of the cell between two optical fibers. After characterization, the cell is flushed back to the outlet 1 by passing through the second set of Tesla's valves (2nd check valve). Developed configuration enables steering of the fluid flow with examined biological material transport with separation of the inlet and outlet.

The fluidic microchannels and microchannels for optical fibers (all 140 μm deep) were etched simultaneously in DRIE process in the 380 μm - thick monocrystalline silicon wafer (Fig. 32a). After etching, 0,3 μm - thick thermal silicon oxide is was formed to passivate chemically surface of the chip. Next, the wafer was anodically bonded (450°C, 1,5 kV) to a borosilicate glass (Borofloat Schott, Germany) with previously mechanically drilled inlet and outlet via - holes. Following, optical fibers with outer diameter of 120 μm and 100 μm core (Ocean Optics, USA) were mounted. Fronts of the fibers were perfectly aligned each to other thanks to high precision of DRIE etching. Fibers were aligned to the edge of microfluidical channel, ensuring immobilization of the oocyte without its mechanical destruction (Fig. 32c). Fibers were fixed by the use of UV NOA 61 epoxy hard glue (Thorlabs, Sweden). Off-chip ends of both fibers were finished with standard SMA 905 connectors compatible with optical connections of the lamp and the spectrometer. Finally, the chip was positioned in a metal package ensuring stable operation during oocyte/embryo management within the chip (Fig. 32b).

The single oocyte/embryo was introduced into lab-on-a-chip by manual pipeting followed by transport of the cell into the measurement cell thanks to capillary forces. After short measurement (circa 5 seconds) of the optical spectra, the biological material was carefully flushed-back to the outlet by applying pressure into the steering port. Then the cell was captured to a sterile transporting container for further treatment.

The measurement set-up consisted of VIS/NIR light source (a halogen lamp by OceanOptics, USA), developed by us lab-on-a-chip, miniature spectrometer (Ocean Optics, USA) and a personal computer with specialized software (this set-up was similar to presented on figure 31).

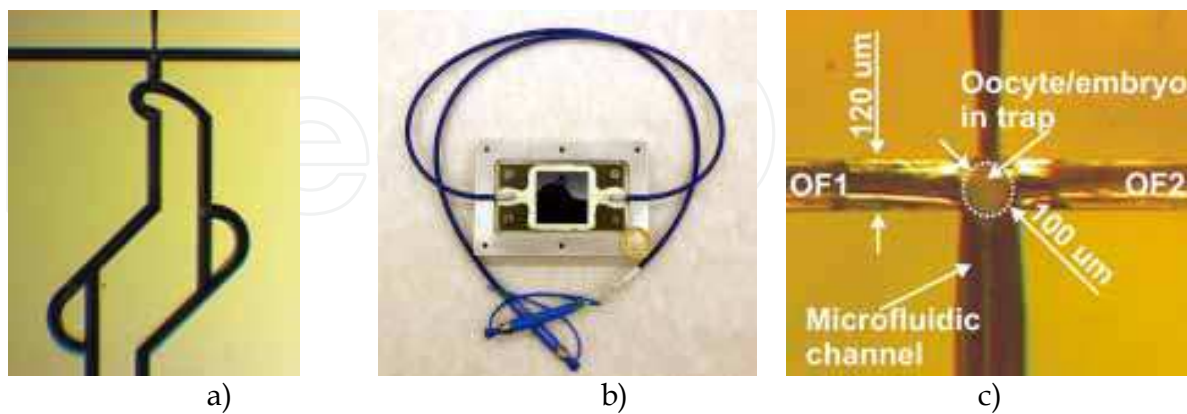


Fig. 32. Lab-on-a-chip for VIS spectrophotometric characterization of oocytes/embryos: a) enlarged view of the silicon chip after DRIE etching - microchannels for optical fibers, measurement cell in the center and Tesla's valves set are visible, b) packaged lab-on-a-chip ready to work in comparison to Polish 2 zloty coin, c) view of the measurement cell with trapped cell (OF1 and OF2 are optical fibers no 1 and 2)

Totally, over five hundreds of porcine and bovine oocytes, as well as almost one hundred of bovine embryos were optically characterized by novel methodology and lab-on-a-chip. Differentiation of collected spectral characteristics of the cells coming from different classification groups (for example ovarian follicle size or morphological properties) has been observed (Fig. 33). On the base of collected data, set of numerical values, describing subjectively optical properties of examined cell, has been proposed: absorbance level for specific wavelength, absorbance ratio for two wavelengths and wavelength position of the absorbance maxima in VIS region.

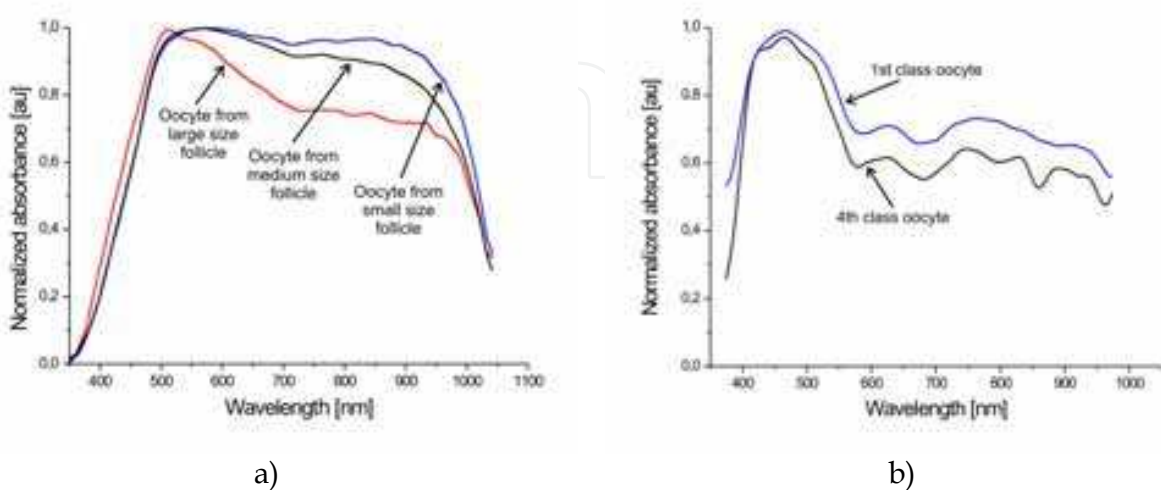


Fig. 33. Example of absorbance spectra obtained for: a) porcine oocytes coming from different sizes of ovarian follicles, b) bovine oocytes for different morphological classes

Further experiments confirmed non-destructive nature of spectrophotometric oocyte characterization. Successful *in vitro* bovine oocyte fertilization after lab-on-a-chip examination has been achieved. This result opens a way towards oocytes selection for artificial fertilization of farm animals oocytes as well as quality assessment of embryos prior to the implantation.

4.3 Fluorometric detector

Labs-on-a-chip dedicated for fluorescence detection of analyte must enable introduction of the fluorescence inducing light and collection of the fluorescence light from an area of interest within the chip. Usually, the chips are whole made of visible light-transparent materials – like glass, PDMS, SU-8, COC or other polymers – or only a top cover of the chip is made of glass, PDMS or other light-transparent materials. Most of the chips are design to co-work with typical apparatus applied for fluorescence induction and readout – epifluorescence microscope (Fig. 34). In this devices, light, usually from arc lamp, light emitting diode (LED) or laser, is restricted to a narrow range of wavelengths that can effectively excitate a fluorochrome and be strongly filtered by the detection channel. The narrow wavelength range is ensured by one or more interference filters and a dichroic mirror. Fluorescence light emitted by the fluorochrome is collected by the microscope objective and guided to a photodetector, passing through filters and dichroic mirror to exclude the excitation light. Common detectors include photomultiplier tube (PMT), semiconductor photodiodes and cooled charge coupled devices (CCD) as sensing matrix in video cameras or lines in spectrometers. Light sources and photodetectors co-work with analog conditioning electronics. The electronic circuits amplify electrical signal with simultaneous reduction of noises. Most of the conditioning electronics is realized by the use of analog circuits. These circuits must ensure high signal to noise ratio (SNR) before the analog signal is digitalized. Therefore, configuration of these analog circuits is sophisticated and only the highest quality elements can be used.

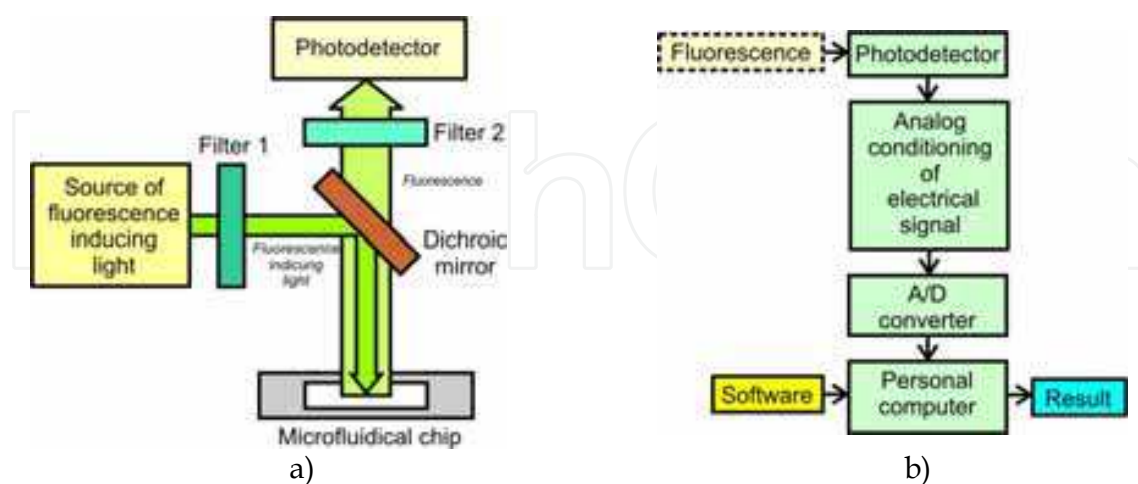


Fig. 34. Fluorescence detection by epifluorescence microscope: a) scheme of the methods, b) path of fluorescence signal conditioning

Although, fluorescence detection is widely used for many years, the configuration of detection apparatus co-working with labs-on-a-chip is based on solutions developed over 20

years ago. Therefore, rapid development of the LOCs must be followed by development of novel methodologies and technical solutions surrounding the chips and leading towards successful application of the microfluidical chips in the point-of-care devices.

In the novel concept of the optical instrumentation for fluorescence induction and readout, application of recent developments in optoelectronics and informatics is involved (Fig. 35).

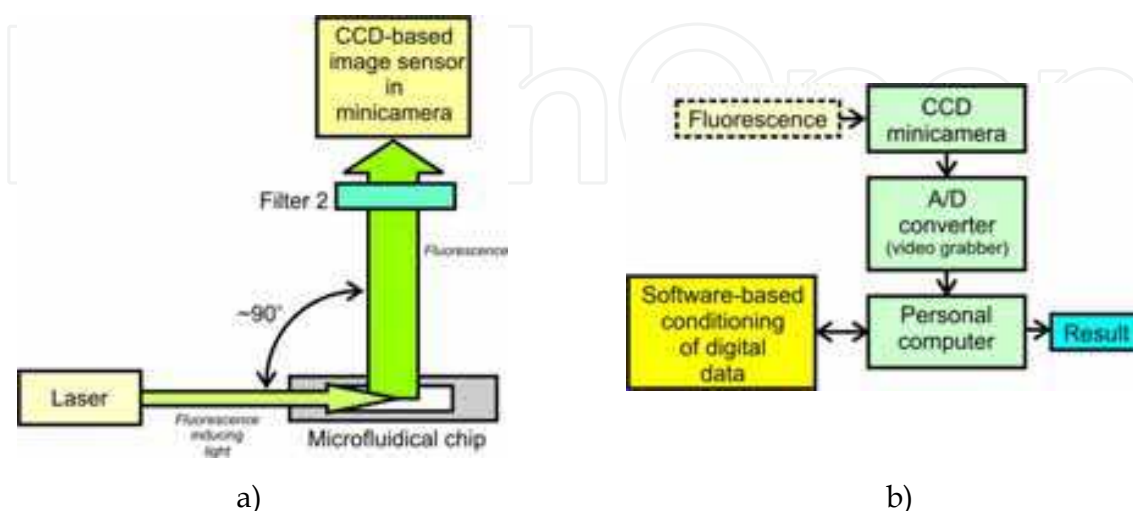


Fig. 35. Fluorescence detection by image sensor and orthogonal configuration of induction/detection channels microscope: a) scheme of the methods, b) path of fluorescence signal conditioning

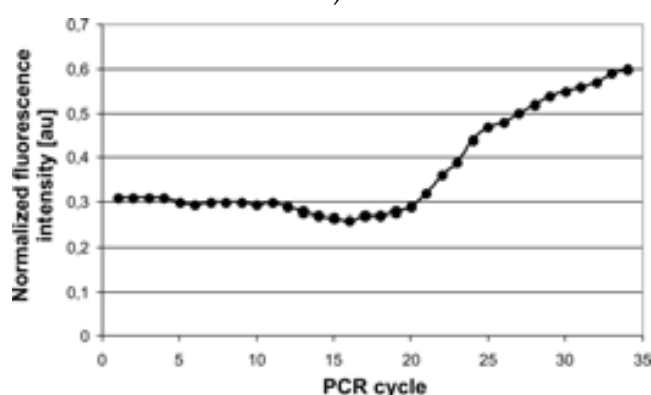
The fluorescence light is induced by a miniature semiconductor laser. Narrow-spectrum of the laser light eliminates application of emission filter. Collimated laser light is introduced - by edge coupling to a light guiding side wall of the chip - directly into detection area of the chip. The view of the detection area containing fluorescence signal is collected by a CCD image sensor being a part of low-cost minicamera module. The detection unit is positioned perpendicularly in relation to the surface of the chip and laser beam. It enables geometrical separation of the laser excitation light and fluorescence signal without application of dichroic mirror, what significantly simplifies the optical part of the detection unit. Therefore, detection unit consist of only one optical filter passing through the fluorescence light and a miniature black/white CCD camera with the objective. The non-conditioned analog output signal from the minicamera is digitalized by one-channel low-cost frame grabber connected to a personal computer (PC). PC stores images in a memory and specialized software carries out analyze of the captured images to give information on fluorescence intensity. Thus, digital conditioning of the fluorescence signal by the software-base image analyze in spite of analog conditioning is applied in the novel concept. Unique feature of the novel methodology is possible re-analyze of the images which are stored in the computer memory. It is not available in typical instrumentation with "non-imaging" photodetectors (PMT or photodiode) when an operator has no chance for the second analyze of carried out experiment.

Novel fluorescence detection methodology and instrumentation co-working with various labs-on-a-chip have been successfully applied in many life-science applications - a portable real-time PCR DNA analyzer, a novel portable cocaine detector, a miniature microcytometer for optical characterization of biosamples or on-chip DNA gel electrophoresis.

One of the most interesting and promising applications of LOCs and presented here fluorescence methodology is portable device for detection of food borne pathogens - *Campylobacter j.* and *Salmonella spp.* by specific amplification of bacteria's extracted DNA with real-time detection of fluorescence - real-time polymerase chain reaction (PCR). This instrumentation has been developed under European project OPTOLABCARD (Ruano-Lopez at al., 2009). The device consists of a disposable real-time PCR chip, a docking station with a specialized chip holder (Fig. 36) and electronics circuits and specialized software for fluorescence signal detection and PCR process temperature profile management.



a)



b)

Fig. 36. Portable real-time PCR DNA analyzer utilizing disposable chips: a) view of the docking station with mounted chip holder, b) typical real-time PCR S-curve of *Campylobacter j.* DNA amplification and detection

The disposable glass/SU-8 chip ($1 \times 1 \text{ cm}^2$) with integrated heater and temperature sensor is placed in a plastic chip holder ($2.8 \times 2.8 \times 0.5 \text{ cm}^3$) with integrated electrical contacts to the chip and some electronics for temperature management. The chip holder has miniature electrical connection to a specialized PCR temperature controller connected to PC. The holder with ready to use chip is positioned in the docking station ($15 \times 5 \times 7 \text{ cm}^3$) in the way ensuring laser light introduction into PCR microchamber and fluorescence light collection. The pre-validation tests of LOC-based system for detection of *Campylobacter j.* were carried out with 48 chicken fecal samples. All the steps - from sample preparation to final result -

were performed in the single chip with 2.5 μl volume of reagents. Red-line fluorochrome (TO-PRO 3) induced by red laser (635 nm, 1 mW) has been applied. The detection unit utilized a long-pass 650 nm interference filter. Typical for real-time PCR fluorescence signal increase during PCR of positive sample has been observed. The ratio of PCR efficiencies between on-chip and on-tube was up to 300%. The sensitivity of on-chip PCR was determined as 0.7-7 ng/ml of template DNA. The real-time PCR process took 30 min – at least 4 times shorter than PCR on-tube.

Similar device but utilizing reusable chip has been developed under Polish national project (Fig. 37). The device was dedicated for rapid detection *E. coli* in water sample. The chip was made of silicon and glass (Fig. 37b). It was passive chip without integrated heater and temperature sensor. PCR temperature profiling was realized by external in relation to the chip Peltier module-based thermocycler. Due to high chemical resistivity of applied chip materials and assembling technique (anodic bonding) it was possible to clean the chip after PCR by the use of standard sterilization processes (chemical or thermal). Thus, the chip was reusable in contrast to the disposable polymer chips.

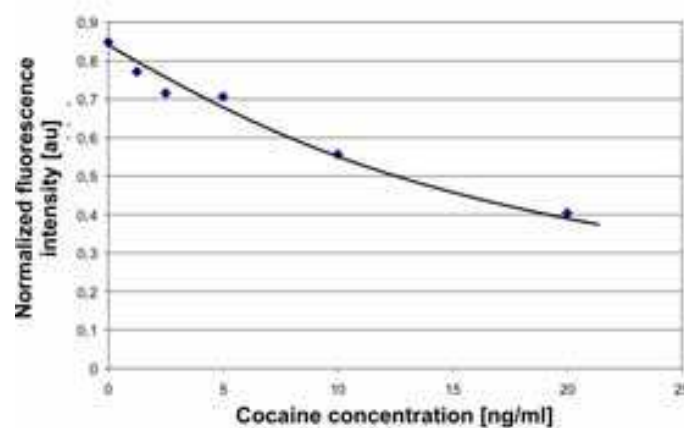


Fig. 37. Desktop real-time PCR device co-working with silicon-glass reusable chips: a) view of the instrument, b) 1 cm x 1 cm chip on author's finger

The second interesting application of the miniature semiconductor laser and CCD-based detection unit is a portable cocaine detector developed under European project LABONFOIL (Walczak et al. 2009). The cocaine test is forecasted to be used as prevention test for professional drivers of heavy trucks or buses. The device consists of a disposable wearable cartridge with implemented biological part for cocaine/metabolite detection in a human sweat sample and a hand-held optical reader connected to a computer. The disposable cartridge contains lab-on-a-paper for sweat sample collection and immunochromatography-based cocaine or its metabolite separation and detection. The hand-held reader utilizes semiconductor red laser diode in the excitation channel and 670 nm interference filter co-working with the minicamera in the fluorescence readout channel. The reader is supplied by USB port of a portable computer (Fig. 38). Preliminary tests of the instrumentation confirmed high sensitivity of the optical reader. Lowest detection limit of the cocaine in sweat sample was better than 2 ng/ml, in comparison cut off of cocaine concentration for simple paper-based test with human eye result readout is well above 100 ng/ml.



a)



b)

Fig. 38. Fluorometric hand-held reader for cocaine test: a) view of the reader connected to a ultra mobile computer with specialized software, b) normalized fluorescence intensity of control line as function of cocaine concentration in the human sweat sample

5. Conclusion

In this chapter chosen examples of physical, chemical and biochemical microsensors, as the discrete element and as a part of the measurement system have been presented. Main design and fabrication problems of miniature sensors, followed by detailed description of measurement systems and instrumentation have been shown. Afterwards, description of tests with presentation of chosen results were presented. It was also clearly shown, that microengineering technology allows to fabricate microsensors - in some cases this technology is the only useful technique enabling integration of the microsensor with the microfluidical device.

During our activities we are trying to follow a rule: "conscious from-chip-to-instrumentation design" what gives measurable effects of well-fitted and unique parts of the microfluidical system. In our opinion it is only way to develop useful microsensors and instruments for microreaction and lab-on-a-chip applications.

6. Acknowledgment

We would like to direct our acknowledgments to Sylwester Bargiel from Université de Franche-Comté (Besançon, France), Jan Koszur, Pawel Kowalski and Bogdan Latecki from Institute of Electron Technology (ITE Warsaw, Poland) for close years cooperation. Special thanks are directed to the members of our group: Patrycja Sniadek, Anna Gorecka-Drzazga, Wojciech Kubicki and Jan A. Dziuban.

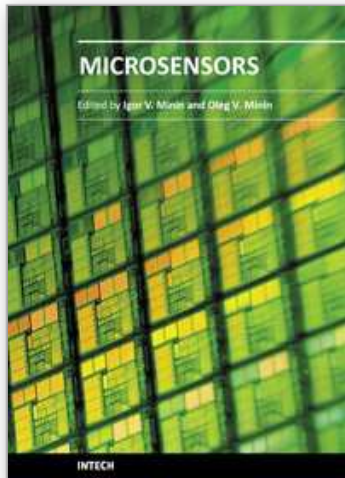
Most of presented solutions were realized under European projects NEPUMUC (FP6), Optolabcard (FP6), Labonfoil (FP7), as well as Polish projects co-funded by European Union – MNS-DIAG/APOZAR and CiS. We would like to thank to for financing our activities and persons realizing those projects for grateful cooperation.

7. References

- Ali, M.F.; El Ali, B.M.; Speight, J.G. (2005). *Handbook of Industrial Chemistry – Organic Chemicals*, McGraw-Hill, ISBN 0-07-141037-6
- Bargiel S.; Górecka-Drzazga A.; Dziuban J. A.; Prokaryn P.; Chudy M.; Dybko A.; Brzózka Z. (2004). Sens. Actuators A, *Nanoliter detectors for flow systems*, No.115, pp. 245-251
- Briand, D.; Weber, P.; de Rooij, N.F. (2004). Sensors and Actuators A, *Bonding properties of metals anodically bonded to glass*, No.114, pp. 543 – 549
- Dietrich, T.R.; Ehrfeld, W.; Lacher, M.; Krämer, M.; Speit, B. (1996). Microelectronic Engineering, *Fabrication technologies for microsystems utilizing photoetchable glass*, No.30, pp. 497 – 504
- Edited by Dietrich, T.R. (2009). *Microchemical Engineering in Practice*, Wiley-VCH Verlag GmbH, ISBN 978-0-470-23956-8
- Dziuban, J. (2006). *Bonding in Microsystem Technology*, Springer, ISSN 1437-0387, ISBN-10 1-4020-4578-6 (HB), ISBN-13 978-1-4020-4578-3 (HB), ISBN-10 1-4020-4589-1 (e-book), ISBN-13 978-1-4020-4589-9 (e-book)
- Ehrfeld, W.; Hessel, V.; Löwe, H. (2005). *Microreactors – New Technology for Modern Chemistry*, Wiley-VCH Verlag GmbH, ISBN 3-527-29590-9
- Freitag, A.; Vogel, D.; Scholz, R.; Dietrich, T.R. (2001). Journal of the Association for Laboratory Automation, *Microfluidic devices made of glass*, Vol.6, Issue 4, pp. 45 – 49
- Knapkiewicz, P.; Walczak, R.; Dziuban, J.A. (2006). *On integration of silicon/glass micromachined sensors to microfluidical devices - toward intelligent microreactor*, Proceedings of XXth Eurosensors Conference, pp. 40-41, ISBN 91-631-9280-2, ISBN 978-91-631-9280-7, Göteborg, Sweden, September 17-20, 2006
- Knapkiewicz, P.; Walczak, R.; Dziuban, J.A. (2007). Optica Applicata, *The method of integration of silicon-micromachined sensors and actuators to microreactor made of Foturan® glass*, Vol. XXXVII, No.1-2, pp. 65 – 72
- Knapkiewicz, P.; Dziuban, J.A.; Boskovič, D.; Loebbecke, S.; Freitag, A.; Dietrich, T.R. (2008). *The system for multipoint pressure and temperature measuring in microreactor used for nitration process*, Proceedings of XXIInd Eurosensors Conference, pp. 40-41, ISBN 978-3-00-025218-1, Dresden, Germany, September 7-10, 2008
- Kralisch, D.; Kreisel, G. (2007). Chemical Engineering Science, *Assessment of the ecological potential of microreaction technology*, No.62, pp. 1094 – 1100
- Ruano-Lopez J.; Agirregabiria M.; Olabarria G.; Verdoy D.; Bang Dang D.; Bu M., Wolff A.; Voigt A.; Dziuban J.; Walczak R.; Berganzo J. (2009). *The SmartBioPhone, a point of*

- care vision under development trough two European projects : OPTOLABCARD and LABONFOIL*, Lab on a Chip 2009, vol. 9, iss. 11, pp. 1495-1499
- Speight, J.G. (2002). *Chemical and process design handbook*, McGraw-Hill, ISBN 0-07-137433-7, United States of America
- Szczepańska P.; Walczak R.; Dziuban J.; Jackowska M.; Kempisty B.; Jaśkowski J.; Bargiel S. (2009). *Lab-on-chip quality classification of porcine/bovine oocytes*, Procedia Chemistry 2009, vol. 1, iss. 1, pp. 341-344
- Walczak R.; Dziuban J.; Szczepańska P.; Scholles M.; Doyle H.; Krüger J.; Ruano-Lopez J. (2009). *Toward portable instrumentation for quantitative cocaine detection with lab-on-a-paper and hybrid optical readout*, Procedia Chemistry 2009, vol. 1, iss. 1, pp. 999-1002
- Zemann A. J. (2001). *Conductivity detection in capillary electrophoresis*, Trends Anal. Chem. 20 6+7, pp. 346-354

IntechOpen



Microsensors

Edited by Prof. Igor Minin

ISBN 978-953-307-170-1

Hard cover, 294 pages

Publisher InTech

Published online 09, June, 2011

Published in print edition June, 2011

This book is planned to publish with an objective to provide a state-of-art reference book in the area of microsensors for engineers, scientists, applied physicists and post-graduate students. Also the aim of the book is the continuous and timely dissemination of new and innovative research and developments in microsensors. This reference book is a collection of 13 chapters characterized in 4 parts: magnetic sensors, chemical, optical microsensors and applications. This book provides an overview of resonant magnetic field microsensors based on MEMS, optical microsensors, the main design and fabrication problems of miniature sensors of physical, chemical and biochemical microsensors, chemical microsensors with ordered nanostructures, surface-enhanced Raman scattering microsensors based on hybrid nanoparticles, etc. Several interesting applications area are also discusses in the book like MEMS gyroscopes for consumer and industrial applications, microsensors for non invasive imaging in experimental biology, a heat flux microsensor for direct measurements in plasma surface interactions and so on.

How to reference

In order to correctly reference this scholarly work, feel free to copy and paste the following:

Pawel Knapkiewicz and Rafal Walczak (2011). Microsensors for Microreaction and Lab-on-a-Chip Applications, Microsensors, Prof. Igor Minin (Ed.), ISBN: 978-953-307-170-1, InTech, Available from:
<http://www.intechopen.com/books/microsensors/microsensors-for-microreaction-and-lab-on-a-chip-applications>

INTECH
open science | open minds

InTech Europe

University Campus STeP Ri
Slavka Krautzeka 83/A
51000 Rijeka, Croatia
Phone: +385 (51) 770 447
Fax: +385 (51) 686 166
www.intechopen.com

InTech China

Unit 405, Office Block, Hotel Equatorial Shanghai
No.65, Yan An Road (West), Shanghai, 200040, China
中国上海市延安西路65号上海国际贵都大饭店办公楼405单元
Phone: +86-21-62489820
Fax: +86-21-62489821

© 2011 The Author(s). Licensee IntechOpen. This chapter is distributed under the terms of the [Creative Commons Attribution-NonCommercial-ShareAlike-3.0 License](#), which permits use, distribution and reproduction for non-commercial purposes, provided the original is properly cited and derivative works building on this content are distributed under the same license.

IntechOpen

IntechOpen